AD-A164 653 MECHANISM OF ELECTROMAGNETIC ENERGY EFFECTS ON THE NERVOUS SYSTEM: VOLTAGE-CLAMP STUDY(U) NAVAL OCEAN SYSTEMS CENTER SAN DIEGO CA C L BRANDT ET AL. JUL 85 1/1

UNCLASSIFIED NOSC/TR-1051 F/G 6/18 NL

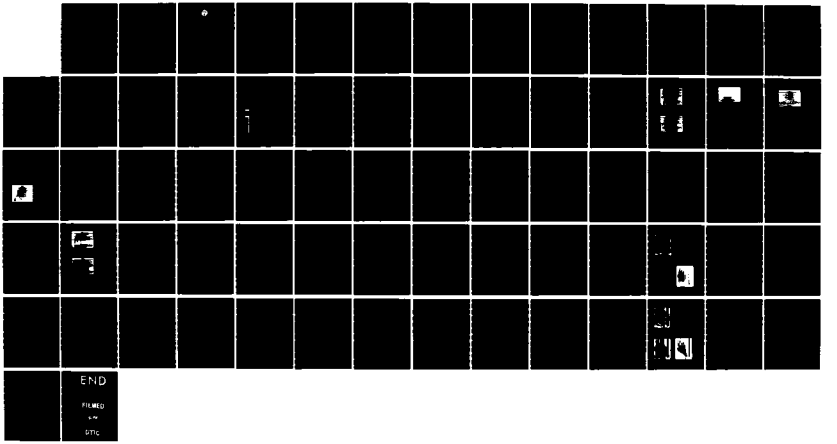

END

FILMED

DTIC

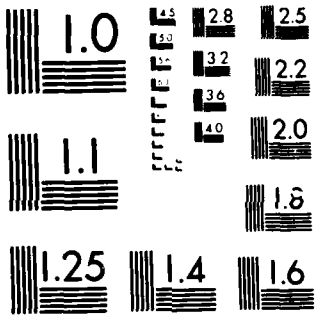

(12)

TR 1051

Technical Report 1051
July 1985

MECHANISM OF ELECTROMAGNETIC ENERGY EFFECTS ON THE NERVOUS SYSTEM: VOLTAGE-CLAMP STUDY

C. L. Brandt
San Diego State University

N. L. Campbell
Naval Ocean Systems Center

Naval Ocean Systems Center
San Diego, California 92152-5000

Approved for public release, distribution unlimited

NAVAL OCEAN SYSTEMS CENTER SAN DIEGO, CA 92152

F. M. PESTORIUS, CAPT, USN
Commander

R.M. HILLYER
Technical Director

ADMINISTRATIVE INFORMATION

The work reported here was performed by members of the Biological Sciences Branch, NAVOCEANSYSCEN, for the Office of Naval Research, Code 441, Arlington, VA 22217.

Released by
L.W. Bivens, Head
Biological Sciences Branch

Under authority of
H.O. Porter, Head
Biosciences Division

UNCLASSIFIED
SECURITY CLASSIFICATION OF THIS PAGE

AD-A164 653

REPORT DOCUMENTATION PAGE

1a REPORT SECURITY CLASSIFICATION UNCLASSIFIED	1b RESTRICTIVE MARKINGS
2a SECURITY CLASSIFICATION AUTHORITY	3 DISTRIBUTION AVAILABILITY OF REPORT Approved for public release; distribution unlimited.
2b DECLASSIFICATION DOWNGRADING SCHEDULE	
4 PERFORMING ORGANIZATION REPORT NUMBER(S) NOSC TR 1051	5 MONITORING ORGANIZATION REPORT NUMBER(S)
6a NAME OF PERFORMING ORGANIZATION Naval Ocean Systems Center 6b OFFICE SYMBOL (if applicable) Code 514	7a NAME OF MONITORING ORGANIZATION
6c ADDRESS (City, State and ZIP Code) Biological Sciences Branch San Diego, CA 92152-5000	7b ADDRESS (City, State and ZIP Code)
8a NAME OF FUNDING SPONSORING ORGANIZATION Office of Naval Research 8b OFFICE SYMBOL (if applicable) ONR-441	9 PROCUREMENT INSTRUMENT IDENTIFICATION NUMBER
8c ADDRESS (City, State and ZIP Code) Physiology Program Arlington, VA 22217	10 SOURCE OF FUNDING NUMBERS PROGRAM ELEMENT NO: 61153N; PROJECT NO: RR04101; TASK NO: 514-MJ15; Agency Accession: DN 288 526

11 TITLE (Include Security Classification)
MECHANISM OF ELECTROMAGNETIC ENERGY EFFECTS ON THE NERVOUS SYSTEM: VOLTAGE-CLAMP STUDY

12 PERSONAL AUTHOR(S)
C. L. Brandt (San Diego State University), N. L. Campbell (Naval Ocean Systems Center)

13a TYPE OF REPORT	13b TIME COVERED	14 DATE OF REPORT (Year, Month, Day)	15 PAGE COUNT
Final	FROM Oct 1981 TO Sep 1984	July 1985	66

16 SUPPLEMENTARY NOTATION

17 COSATI CODES			18 SUBJECT TERMS (Continue on reverse if necessary and identify by block number)
FIELD	GROUP	SUB GROUP	Microwave energy, voltage clamping, firing frequency, neuronal activity, Aplysia californica neurons, ionic currents, microelectrodes, ganglion, Stimulus Isolation Units (SIU)

19 ABSTRACT (Continue on reverse if necessary and identify by block number)

Low-level microwave energy at a frequency of 2.45 GHz has been previously observed to alter the firing frequency of Aplysia californica neurons. This study was undertaken to search out the mechanism of this microwave effect by examining the influences of microwave energy on specific ion currents across the cell membrane that influence the cell's firing frequency. Late outward K^+ current was examined and showed no statistically significant change during microwave exposure. The membrane current shape during voltage clamping (the summation of several different ionic currents) also showed no change during exposure except in one instance when exposure was concurrent with the application of Na^+-free artificial sea water.

20 DISTRIBUTION AVAILABILITY OF ABSTRACT	21 ABSTRACT SECURITY CLASSIFICATION	
☐ UNCLASSIFIED UNLIMITED ☒ SAME AS RPT ☐ DTIC USERS	UNCLASSIFIED	
22a NAME OF RESPONSIBLE INDIVIDUAL N. L. Campbell	22b TELEPHONE (Include Area Code) (619) 225-7372	22c OFFICE SYMBOL Code 442

DD FORM 1473, 84 JAN

83 APR EDITION MAY BE USED UNTIL EXHAUSTED
ALL OTHER EDITIONS ARE OBSOLETE

UNCLASSIFIED
SECURITY CLASSIFICATION OF THIS PAGE

EXECUTIVE SUMMARY

PROBLEM

Low-level microwave energy at a frequency of 2.45 GHz has been previously observed to alter the firing frequency of Aplysia californica neurons. This study was undertaken to search out the mechanism of this microwave effect by examining the influence of microwave energy on specific ion currents across the cell membrane that influence the cell's firing frequency.

RESULTS

Late outward K^+ current was examined and showed no statistically significant change during microwave exposure. The membrane current shape during voltage clamping (the summation of several different ionic currents) also showed no change during exposure except in one instance when exposure was concurrent with the application of Na^+-free artificial sea water.

CONTENTS

FIGURES

FIGURES (Continued)

TABLES

INTRODUCTION

PROBLEM

Exposure to 2.45-GHz energy in the power density range of 10 to 300 mW/cm^2 (SAR range of 2 to 60 mW/g) has been shown to produce a change in firing frequency of Aplysia neurons in 11% of the exposed cells (Campbell and Brandt, 1982). Other findings likewise suggest a microwave influence on neuronal activity (Wachtel et al., 1975; Seaman and Wachtel, 1978; Arber, 1981; Arber and Lin, 1982; 1983; Lin and Arber, 1982; Sheppard and Adey, 1982). The mechanism of this apparent interaction of microwave exposure and neuronal activity is now of interest. Neuronal activity is heavily controlled by the cell membrane, which selectively allows the passage of charged ions. This study is an examination of microwave influence on some aspects of membrane activity.

BACKGROUND

Much is already known regarding the membrane-associated mechanism of neuronal activity. For example, individual Aplysia californica neurons have been identified by their autoactive behavior--self-generated action potentials at frequencies and patterns characteristic of the cell (Arvanitaki and Chalzonitis, 1963; Frazier et al., 1967; Connor and Stevens, 1971). The frequency and pattern of these action potentials are determined by the interaction of at least five different ionic currents that enter or exit the neuron (Adams et al., 1980). These ionic currents vary in magnitude over time because of a time-dependent membrane conductance for each individual ion species. The ion-specific membrane conductance is controlled by membrane potential, neurotransmitters, and intracellular agents. An example of the latter mechanism is the activity of photosensitive neurons. Exposure of these cells to visible light releases Ca^{++} from intracellular storage sites. The resulting increase in intracellular Ca^{++} concentration causes an increase in membrane conductance to K^+. Potassium ions flow out of the cell, resulting in hyperpolarization and decreased firing frequency (Andresen and Brown, 1979).

A microwave-induced alteration of firing frequency may result from a direct influence on the ion channels in the membrane, or from an indirect effect on other agents, which in turn control the membrane conductance. To monitor changes in the membrane conductance, the technique of voltage clamping was used.

Two microelectrodes are inserted into a neuron. One microelectrode serves to monitor the membrane potential while the other serves as a current-passing electrode. A differential amplifier compares the membrane potential with a command potential and, if these potentials differ, injects a current into the cell to bring its potential to that of the command. The current required to do this reflects the ionic currents flowing across the membrane in response to the changed membrane potential. This current is monitored. An alteration in the ionic current response during microwave exposure would explain the previously observed alteration of firing frequency. Specifically, since the previous findings indicated an inhibition of firing, we anticipated seeing an increase in membrane conductance to K^+ during exposure.

APPROACH

The goals of this study were as follows:

1. Develop a voltage-clamp system capable of clamping Aplysia neurons during microwave exposure;

2. Observe changes in total membrane current during voltage clamping under exposure conditions, especially changes in that part of the current carried by K^+; and

3. Determine the ionic basis for any observed microwave-induced changes in total membrane current.

MATERIALS AND METHODS

Much of the equipment and many of the procedures used in these voltage-clamp experiments were also used in the previous experiments to monitor firing frequency, and are described in detail in NOSC TR 698 (Campbell and Brandt, 1982). A summarized version of the original system, along with any changes and/or additions, will be detailed here.

PROCUREMENT AND MAINTENANCE OF APLYSIA CALIFORNICA

Aplysia californica, 100 to 300 g, were purchased from Pacific Biomarine (Venice, CA) or collected from local tidepools and maintained in a 15-to-17°C sea water aquarium (Oceanic 35/35, Jewel Industries, Inc., Chicago, IL). The animals were fed every other day with Romaine lettuce leaves and dried red algae (Mushibi Nori, Japan Food Corp., San Francisco, CA).

The aquarium was equipped with a supplemental oyster shell filter, which maintained the sea water quality for 2 weeks or more. Bacteria attached to the oyster shell and grew by feeding on organic material in the sea water, thus maintaining water quality. The shell also served to maintain the pH of the water in an appropriate range.

The filter consisted of an 11-gallon polyethylene tank fitted with a fiberglass screen-covered, perforated, false bottom. The false bottom supported a 6-inch-deep bed of crushed oyster shells. Two identical pumps (Model IA-MD, March Manufacturing Co., Glenview, IL) moved sea water from the main aquarium onto the top of the filter bed and from the bottom of the shell bed back into the main aquarium. Every 6 weeks, the filter was backflushed with tap water followed by sea water to remove accumulated bacteria.

The filter was connected to the main aquarium with a siphon and overflow constructed of 3/4-inch plastic pipe. The piping prevented loss of water from the main aquarium in case of power failure. Two air stones in the main aquarium were supplied by an aquarium air pump.

GANGLION PREPARATION AND MAINTENANCE

At the start of an experiment, the abdominal ganglion of an Aplysia was dissected out and pinned to the Sylgard base of the exposure chamber (see fig 1) with cactus spines. The insertion of two microelectrodes into one cell required careful removal of connective tissue over the cell. This was accomplished by using fine-tipped forceps (DuMont #5) sharpened to a chisel point to grip the connective tissue to one side of the ganglion. A piece of razor blade (Gillette Platinum-Plus) held in a bent hemostat was then used as a microscalpel to slice the tissue away from the cells, allowing unobstructed insertion of two microelectrodes.

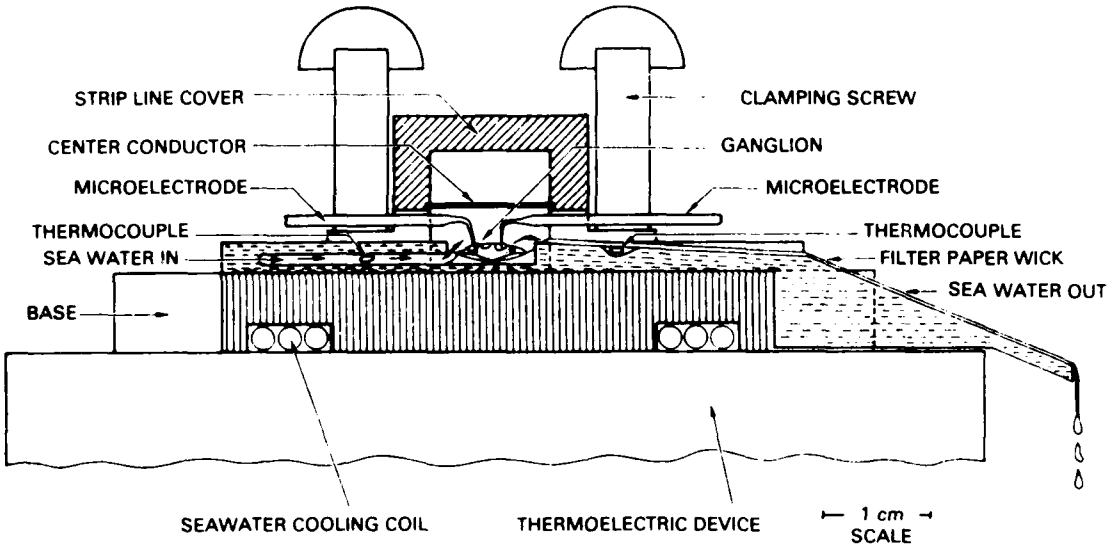

Figure. 1. Cross-section diagram of exposure system.

Cooled sea water was suffused over the ganglion throughout the experiment to maintain it in a healthy state. The inlet and outlet temperatures of the sea water were monitored on a Thermalert Digital Thermometer (Model TH-6D, Baily Instrument, Saddle Brook, NJ) and recorded on a chart recorder. The baseplate of the stripline was maintained at a constant temperature by a thermoelectric device (Cambion Model 806-1002-01-00-00) controlled by a Cambion Model 809-3030-01 Bipolar Controller (Cambion Thermionic Corp., Cambridge, MA).

The suffusion system contained about 2 liters of sea water in the reservoir and connecting tubing. This large volume added a capacitance to the system that slowed the settling time of the capacitive current. To minimize this capacity and provide a means of rapidly changing from one suffusion fluid to another, a manifold with air traps was constructed. Figure 2 illustrates the valve manifold and air traps. The unit was constructed of three-way stopcocks (Pharmaseal K75, Toa Alta, Puerto Rico) and air traps from intravenous infusion systems. The Teflon needle valve (Manostat Model 08-425-001, New York, NY) regulated the flow through the suffusion chamber. Drop counting gave an indication of flow rate, one drop being approximately 65 microliters. Typical flow rates were 20 to 40 drops per minute. Since the empty exposure chamber held about 140 microliters of sea water, these flow rates exchanged the fluid in the chamber eight to 16 times per minute.

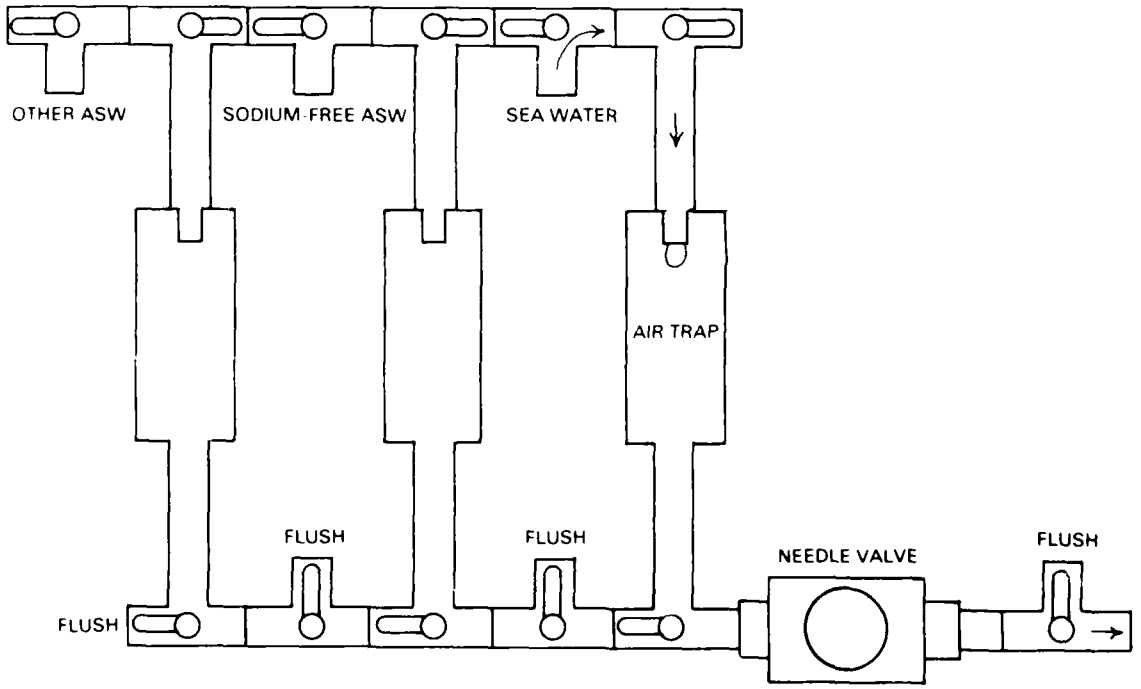

Figure 2. Valve manifold and air traps.

MICROELECTRODE PREPARATION

Microelectrodes were pulled on a vertical pipette puller (Model 700C, David Kopf, Tujunga, CA) from 4-inch lengths of microelectrode glassware 1.5 mm in outside diameter (No. 1B150F, W-P Instruments, Inc., New Haven, CT). After pulling, the lower microelectrode was moved back into the puller's heating coil and bent to a right angle. The length of the bent tip, from the outside edge of the untapered portion of the glass tubing to the tip, was 3.4 to 3.8 mm. This length restriction, while severe, was necessary to prevent the electrode shank from touching the irradiation fixture cover or contacting the suffusion water in the outlet channel. After pulling and bending, the microelectrodes were placed on a plastic holder and immersed, tip end down, in 3-M KCl that had been filtered through a membrane filter with 0.2-μm pores. The microelectrodes filled overnight by capillary action.

Suitability of the microelectrodes for use in an experiment was determined by measuring the electrical resistance of the microelectrode when mounted in series with two Ag-AgCl electrodes, a 3-M KCl salt bridge, and a multimeter with an analog display. A resistance in the range of 3 to 7 MΩ indicated a tip diameter in the range of 0.5 μm, a size that penetrates neurons easily with a minimum of trauma to the cells. Microelectrodes in this resistance range were used to monitor membrane potential, but were not suitable for the current-passing electrode.

For passing sufficient current to clamp a cell rapidly without "ringing," microelectrodes with resistances in the range of 0.6 to 1.2 MΩ were required. Several methods of fabricating these low-resistance pipettes were tried before a satisfactory method was found. First, by altering the heating and solenoid currents on the pipette puller, microelectrodes within the low-resistance range could be obtained. However, these electrodes did not penetrate cells easily and routinely came out of the cells within a few minutes. It is possible that the difficulties were attributable to the sharper taper of the tip of these electrodes.

Second, attempts were made to bevel microelectrode tips. A microelectrode beveler was assembled according to the method of Ogden et al. (1978). In this technique, the tip of a KCl-filled microelectrode was inserted at a 45-degree angle into a pressure-driven fine stream of 3-M KCl containing an abrasive (0.05 μm gamma-alumina, Buehler Micropolish). The microelectrode resistance was monitored continuously and when it dropped to about 1 MΩ from the 4- to 7-MΩ range (about 3 minutes), the microelectrode was withdrawn. Beveled pipettes penetrated cells easily and passed sufficient current to get good clamps. However, cells penetrated with beveled microelectrodes did not seem to recover well from the penetration, so this method was discontinued. It was found eventually that microelectrodes pulled to the range of 4 to 7 MΩ could be broken to yield around 1 MΩ by gently touching the tip to a piece of clean tissue. These microelectrodes penetrated cells easily, did not prevent cell recovery, and often remained in the cell for four or more hours. This technique was used on current-passing electrodes for most experiments done after February 1983.

Note that the amplifiers used to monitor the neuroelectrical signal have a microelectrode resistance-measuring circuit. It was found that electrode resistances measured on the multimeter were about 50% lower than those measured on the amplifier. All microelectrode resistances reported here are those measured on the multimeter.

MICROELECTRODE HOLDERS AND REFERENCE ELECTRODE

The microelectrode holders and reference electrode in these experiments used Ag-AgCl electrodes. The holders were modifications of versions purchased commercially (No. MEH2S15, W-P Instruments, Inc., New Haven, CT) and described in NOSC Technical Report 698 (Campbell and Brandt, 1982). After each day's use, the holders and reference electrode were rinsed with distilled water, blown dry, and stored in a desiccator. Electrode holders were replaced about every 4 to 5 weeks, when they began developing potentials greater than 4 mV and/or showed electrical instability.

CELL IMPALEMENT AND SIGNAL MONITORING

Two high-impedance DC amplifiers, (Model M-707, W-P Instruments, Inc., New Haven, CT) were used to monitor the cell's electrical activity. Prior to cell impalement, holders carrying microelectrodes of the proper resistance were mounted on micromanipulators (Model CP-V, Brinkman Instrument, Inc., Westbury, NY) and attached to the amplifier probes. The microelectrodes were then advanced into the suffusion fluid covering the desheathed ganglion and tested for tip potential and resistance. Newly pulled electrodes occasionally had potentials as high as 60 mV and could not be used. Usually, however, tip potentials were of the order of 4 to 6 mV and stable. These tip potentials were balanced out with the offset potential source in the amplifiers. Occasionally, both electrodes showed an identical potential of the order of 10 to 200 mV, indicating either a faulty reference electrode or the presence of a chemical potential arising from the leakage of sea water onto the aluminum baseplate of the irradiation fixture. In either case, the fault was found and corrected before cell impalement proceeded.

The microelectrodes were advanced toward a cell through the suffusion fluid and oriented as far apart as possible over the chosen cell. To increase the electrode separation, the micromanipulators were permanently tilted 7 degrees off normal in opposite directions, forward and backward. Contact of the electrode with the cell surface (or the connective tissue above it) was announced by the changed pitch of an audible baseline monitor (ABM, W-P Instruments, Inc.). Each microelectrode was then advanced independently or simultaneously until one or the other penetrated the cell. Penetration was signaled by the sudden appearance of a potential of the order of -20 to -50 mV, often accompanied by spontaneous firing of action potentials. The other electrode was then advanced until penetration. The membrane potential recorded from the first electrode often dropped to about one-half its initial value upon penetration of the second electrode. Successful impalement was indicated by identical electrical activity from both microelectrodes, as monitored from each amplifier.

Hyperpolarizing pulses of constant current aid cell recovery from electrode insertion. The shape of the membrane potential response to the pulses provides a measure of cell health. In these experiments, constant current pulses were provided by a stimulator (Model 302-T, W-P Instruments) via a stimulus isolator (Model 1880, W-P Instruments). The pulses were passed through a bridge circuit on the amplifier attached to one of the electrodes. The pulses were adjusted to give 1-second hyperpolarization to about -80 mV at 3-second intervals. Pulsing was continued for up to 10 minutes until the membrane potential changes induced by the pulsing stabilized. The cell was then allowed to recover for 30 to 90 minutes before clamping was begun. Electrical activity from both electrodes was recorded continuously during this period on a chart recorder.

IDENTIFICATION OF NEURON AND/OR NEURON FIRING PATTERN

The period of recovery after cell impalement and before voltage clamping served to confirm the identity of the impaled cell according to the nomenclature of Frazier et al. (1967). They found that a number of Aplysia abdominal ganglion neurons could be distinguished as individual types that occur in every animal and thus could be named. The identification of each named cell was based on its size, location in the ganglion, pigmentation, response to certain neurotransmitters, membrane potential, and firing pattern.

Where it was not possible to identify an impaled cell with certainty in our experiments, it was classified according to its firing pattern as a beater, burster, or silent cell. Figure 3 illustrates the firing pattern of three cells, each fitting one of these categories. As can be seen from the figure, a beating cell spontaneously fires action potentials at fairly regular intervals, interrupted only occasionally by synaptically driven changes in frequency. A bursting cell fires two or more action potentials in a burst followed by a long period of hyperpolarization, then another burst, and so on. A silent cell fires only an occasional action potential, or none at all.

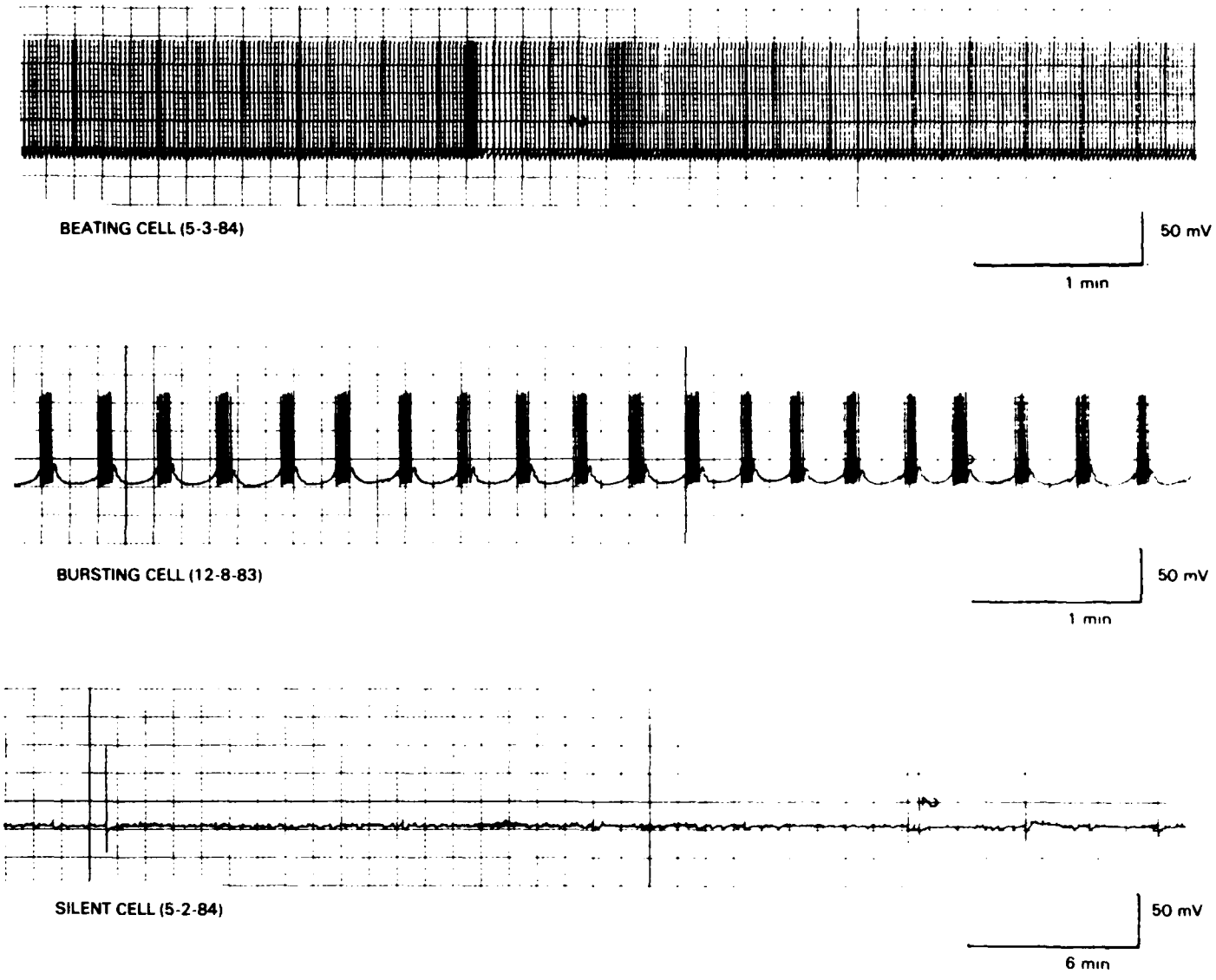

Figure 3. Neuron firing patterns.

MEASUREMENT OF INPUT RESISTANCE

According to Kandel (1976, p 113), the input resistance (R_i) of neurons ranges from 10^5 to 10^9 Ω. Other laboratories (Andresen, University of Texas Medical Branch, Galveston, TX; personal communication) use the value of 1 MΩ or greater to indicate that an impaled Aplysia neuron is "healthy." Input resistance was measured by determining the voltage drop produced across the cell membrane by a pulse of known constant current. Current pulses from the stimulators were fed into the current input of the amplifier and out through one of the electrodes. The size of the current pulse was measured from the current monitor output of the amplifier as a voltage drop and recorded on a chart recorder. The voltage drop across the membrane (V_m) was monitored by the other electrode-amplifier combination and recorded on the chart recorder. The input resistance then was calculated by:

$$R_i = \frac{I}{V_m} .$$

In the early stages of this work, R_i was routinely determined.

VOLTAGE-CLAMP APPARATUS

The purpose of voltage clamping is to determine the nature and time course of the currents flowing through a cell's membrane in response to voltage changes, neurotransmitters, pharmacological agents, etc. A diagram of the essential elements of a voltage clamp is given in schematic form in figure 4. As shown, a cell bathed in sea water was impaled with two microelectrodes. One microelectrode was attached to a high-impedance amplifier that monitored the cell's membrane potential (V_m). The V_m was displayed on an oscilloscope and provided one input to a differential amplifier, which compared the V_m with a command signal [a steady DC holding potential (V_h), upon which square-wave pulses were superimposed]. If the command signal and V_m differed, a current (I_m) was passed into or from the cell through the second microelectrode to bring V_m equal to the command. A current-to-voltage converter produced a voltage output that was proportional to the current.

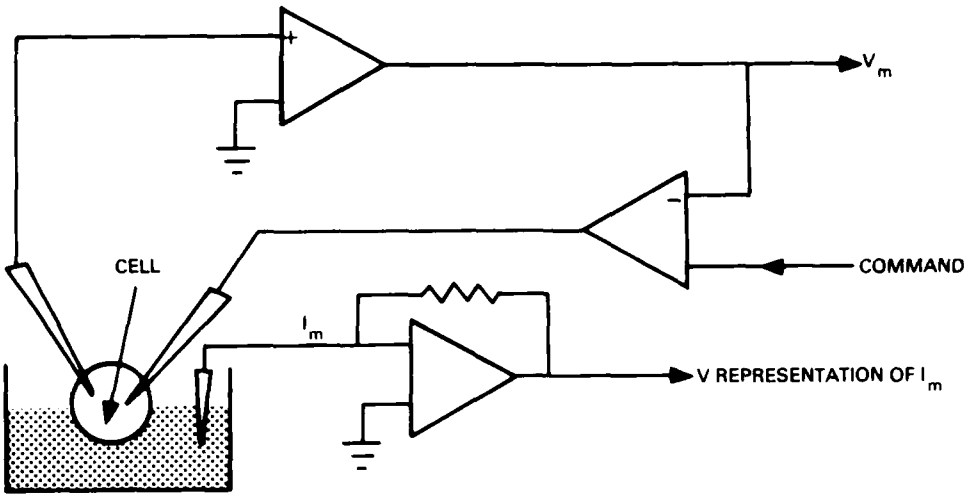

Figure 4. Voltage-clamp block diagram.

Figure 5 illustrates a cell's expected response to voltage clamping; in this example, the command signal pulses from a -50-mV holding potential to +30 mV. This pulse is held for at least 80 ms. The membrane potential follows the command signal, indicating a successful clamp. The membrane current tracing illustrates the cell's response to this manipulation of its membrane potential. At the holding potential, the current (I_m) is defined as zero. During the pulse, I_m shows three phases. First, a very rapid outward current, which represents the discharge of the cell's membrane capacitance. This capacitive discharge may also reflect capacitance in other parts of the electronic circuit. Second, following the settling of the capacitive current, the I_m reflects a flow of positive charges into the cell--an inward current carried primarily by sodium ions (Na^+). This inward current results from the transient opening and closing of Na^+ channels in the membrane. Third, an outward current appears that is maintained for the duration of the positive pulse and reflects the opening of potassium ion (K^+) channels, allowing K^+ to flow out of the cell. Figure 6 is a block diagram of the present configuration of instruments in the voltage clamp used in the study described in this report. The neuron cell body (soma) is represented in a fluid-filled chamber (exposure chamber) impaled with two microelectrodes. Silver-silver chloride (Ag-AgCl) reference electrodes connected the microelectrodes to probes from the M-707

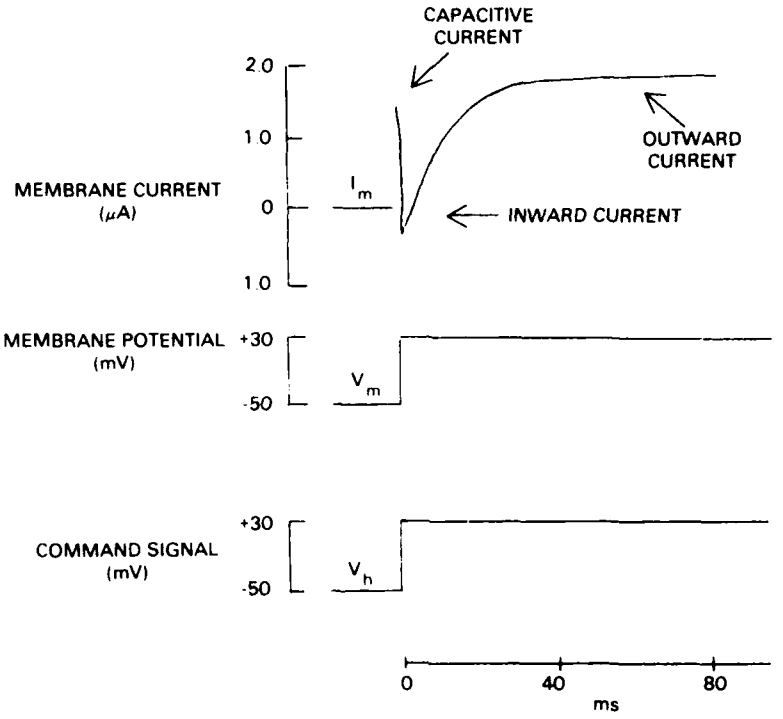

Figure 5. Cell's response to voltage clamping.

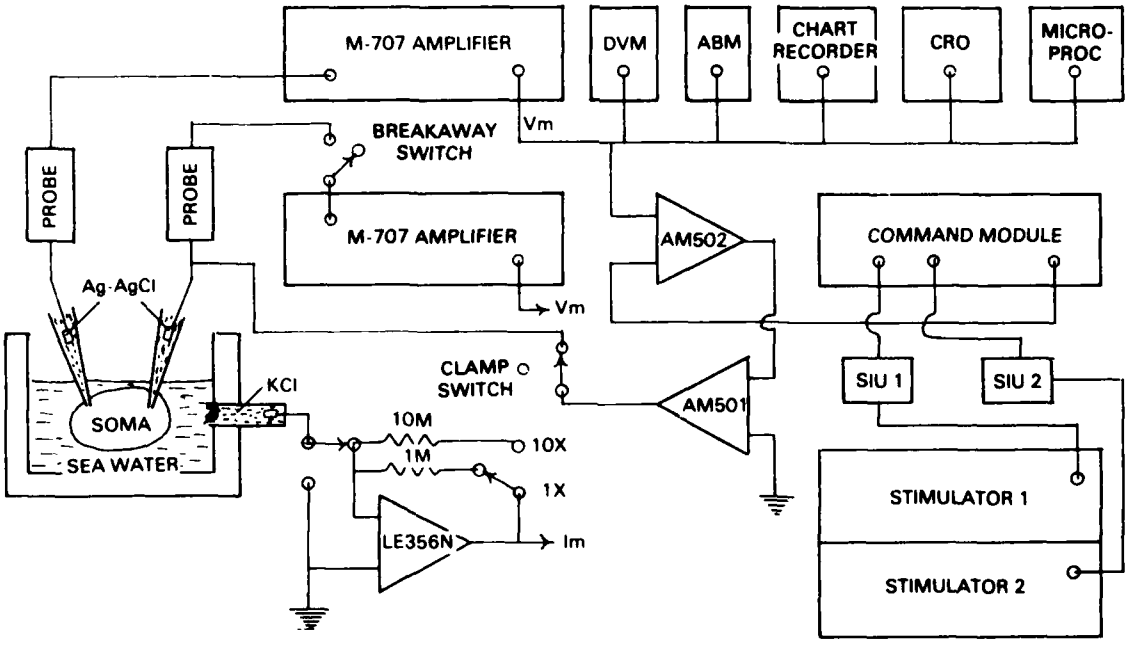

Figure 6. Block diagram of voltage-clamp apparatus.

amplifiers. One M-707 amplifier monitored the V_m. The output of this amplifier was observed on a digital voltmeter (DM501A Digital Multimeter, Tektronix, Inc., Beaverton, WA), listened to on an audible baseline monitor, recorded on a four-channel recorder (Model 2400, Gould Instruments, Inc., Cleveland, OH), viewed on a storage oscilloscope (Tektronix, Model 5111A), and sent to a microprocessor (developed in-house). The V_m from this amplifier also served as one input to the differential amplifier (Tektronix AM502). The other M-707 amplifier also monitored V_m when pipettes were first inserted into the cell. During voltage clamping, however, this amplifier and its probe were bypassed by opening the breakaway switch and closing the clamp switch (as shown).

The command module supplied the holding potential and superimposed the voltage pulses output by the stimulus isolation units. The command module output was sent to the differential amplifier. The output of the differential amplifier was increased by an operational amplifier (Tektronix AM501) and sent to the current-passing microelectrode, bypassing the probe when the clamp switch was closed (as shown). The current flowing through this microelectrode and the cell membrane was converted to a proportional voltage by the current-to-voltage converter, viewed on the oscilloscope, and sent to the microprocessor.

GENERATION AND CONTROL OF THE COMMAND SIGNAL

The command signal to the differential amplifier was issued by the command module. The circuit for the command module was modified by P. Hayes (NOSC, Code 523) from one used in A. M. Brown's Laboratory at the University of Texas Medical Branch and is shown in a simplified diagram in figure 7. The unit consisted of a summing amplifier, which summed the modified input from three pulse input channels, and an internally generated DC voltage into one output signal, the command signal. Each input channel received the output from one stimulus isolation unit (SIU). Each SIU was driven by a separate stimulator. The stimulators controlled the duration, frequency, and delay of pulses output from the SIUs. The amplitude of the DC pulses from the battery-powered SIUs was controlled by a potentiometer on the SIU. In most of the experiments reported here, single pulses of different magnitudes were applied

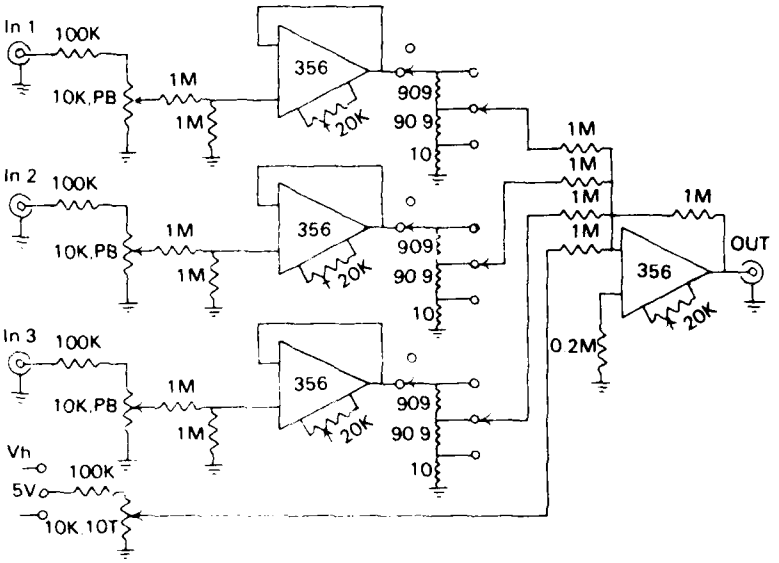

Figure 7. Circuit diagram of command module.

to a voltage-clamped cell; hence only a single stimulator and SIU were used. In a few experiments, a hyperpolarizing pulse was delivered to the clamped cell just prior to a depolarizing pulse. In these cases, the outputs of two stimulator-SIU combinations were summed.

The output of the command module was adjusted as it was viewed on the oscilloscope, which was itself triggered by the stimulator. First, the internally generated DC voltage was divided by a 10-turn potentiometer mounted on the outside of the command module to give a -50-mV output. This constituted the holding potential. The SIU was then turned on and the duration of the pulse from the stiumlator was adjusted to 45 or 85 ms [corresponding to the oscilloscope resolution (5 or 10 ms/div) desired to monitor the membrane's current response to voltage clamping]. A pushbutton potentiometer, also mounted on the outside of the command module (one for each input channel), manipulated the amplitude of the pulse from the SIU before the pulse was input to the summing amplifier. This potentiometer was set at 110 and the output of the SIU was adjusted by using its potentiometer to give a pulse of 20 mV, thus

calibrating the output of the command module to give a 20-mV increment in voltage for each 110 units on the pushbutton potentiometer. The calibration was checked at several higher pushbutton settings; for example, a reading of 440 would show a pulse amplitude of 80 mV. Polarity of the pulse was determined by a switch on the SIU.

DIFFERENTIAL AMPLIFIER AND CURRENT GAIN

A Tektronix AM502 differential amplifier initially served as a current source in this system. Early tests indicated that the 5-V output of this amplifier was insufficient to produce an acceptable V_m rise time (less than 1 ms to reach a command pulse of +25 mV). An amplifier with a gain of two was constructed and added to the output of the AM502. Figure 8a indicates that even with this additional gain, the rise time was about 2 ms. A Tektronix AM501 operational amplifier capable of outputting 40 V was added. Figure 8b shows that the rise time of the membrane potential improved to less than 0.1 ms, which was acceptable for this work.

This description of the rise time of the membrane potential when voltage clamped raises the question of how fast the different components of the voltage-clamp system responded. Figure 9 is a photograph of the storage oscilloscope displaying the output from two points in the system that corresponded to a 20-mV pulse from the command module. The sweep speed is 0.2 ms/division. The lower trace is the output of the SIU pulse (4V) going to the command module. Time for the SIU pulse to reach 95% of its full value is about 0.05 ms. The middle and top traces are the output of the command module and the output of the V_m monitoring amplifier, respectively. Rise time for both signals is approximately 0.05 ms.

In voltage clamping a cell, the gain of the differential amplifier must be sufficient to supply a signal that brings the membrane potential rapidly to the desired value and holds it there without fluctuation. The feedback gain must not be so high as to cause ringing (fluctuations of V_m around the desired potential with gradual damping). To initially get the gain in the correct range, a hyperpolarizing pulse was delivered at a slow repetition rate to

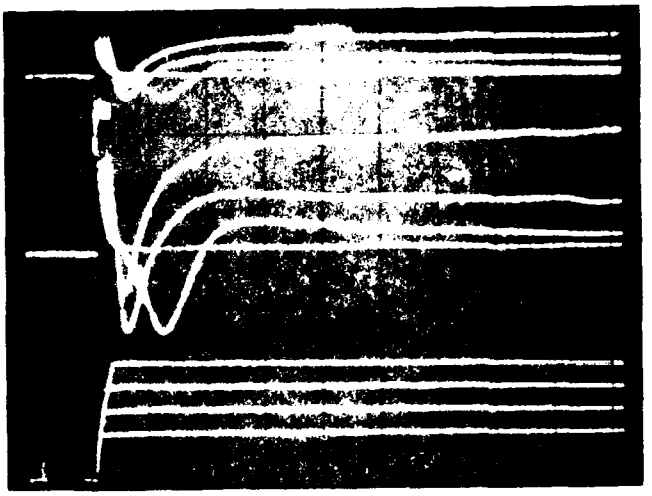

COMMAND (5 V/div)

I_m (0.5 V/div)

V_m (50 mV/div)

a. Clamp using differential amplifier output limited to ±10 V

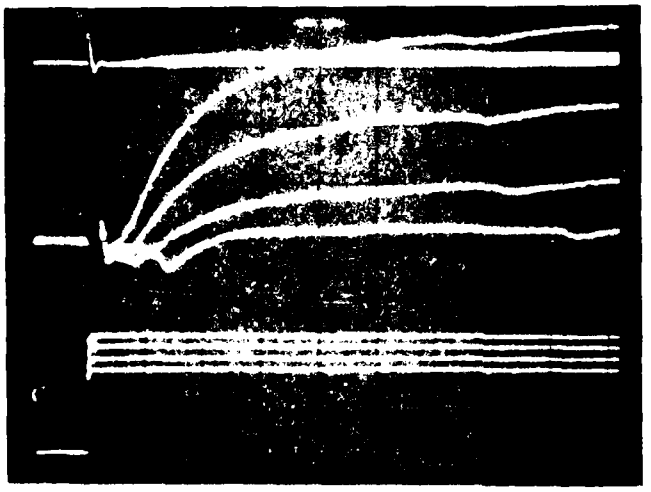

COMMAND (5 V/div)

I_m (0.5 V/div)

V_m (50 mV/div)

a. Clamp using differential amplifier output limited to ±40 V

Figure 8. Effect of increase in output of differential amplifier.

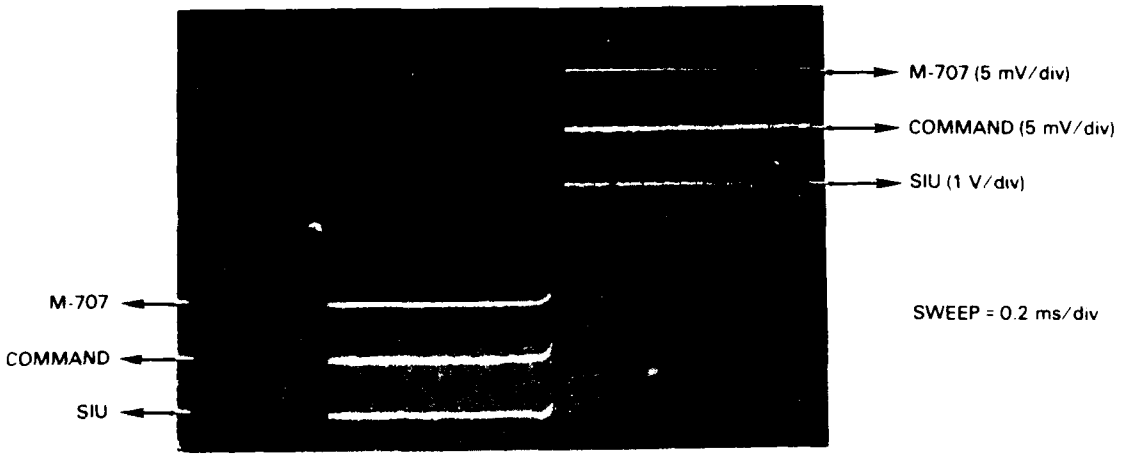

Figure 9. Rise-time determination.

clamp the cell at about 40 mV below the -50-mV holding potential (-90 mV total). The gain on the AM502 was increased to produce the squarest waveform possible without ringing. The filtering on the AM502 also was increased to get the best waveform. For most Aplysia neurons clamped, a gain of 2K or 5K with a filter setting of 1 kHz or 3 kHz gave the best results. Ringing was also minimized by using low-resistance (0.6- to 1.2-MΩ) electrodes (see Microelectrode Preparation, above).

Because of the high gain used on the differential amplifier, it was important that the electronics add as little noise as possible to AM502 input signals (V_m and command). The top trace in figure 10 shows the output of the V_m monitoring M-707 at an oscilloscope setting of 1 mV/division. The noise from this source was less than 0.1 mV. However, the output of the command module, third trace from the top, shows a high-frequency noise of greater than 0.1 mV (broadening of the trace) and a 60-Hz component of about 0.4 mV peak to peak. This noise is generated in the command module since the ouput of the SIU (second trace from the top) shows little high-frequency noise and only a small 60-Hz component. It was surmised that a battery supply to the command

module would improve the signal-to-noise ratio. However, this change was not made, so all records reported here reflect the inherent noise from this source.

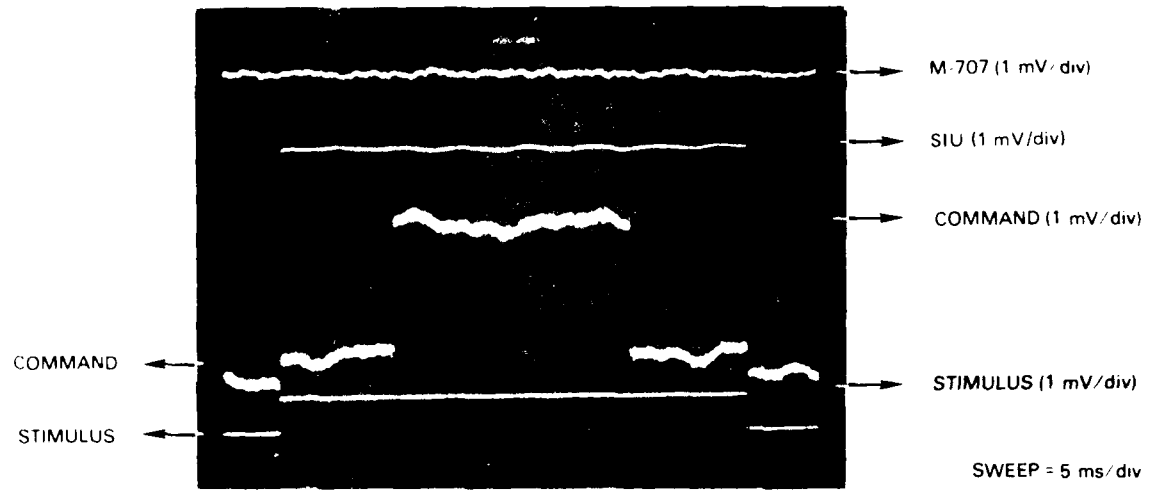

Figure 10. Noise determination.

CURRENT-TO-VOLTAGE CONVERTER

Figure 11 shows a simplified circuit of the current-to-voltage (I/V) converter modified by P. Hayes (NOSC, Code 523) from a design furnished by A. M. Brown (UTMB, Galveston, TX) and used in all the work reported here. A gain of one on the I/V converter was used throughout.

The voltage representations of the currents obtained from the I/V converter were displayed on the oscilloscope screen in the storage mode and were photographed on Polaroid P107 or 667 film with a Tektronix C5 camera (Tektronix, Inc., Beaverton, WA). Figure 12 is an example of a set of data photographed during a typical clamp series. The top traces display seven superimposed membrane potentials to which the cell was pulsed at successive 15-second intervals from a V_h of -50 mV. The lower traces are the superimposed

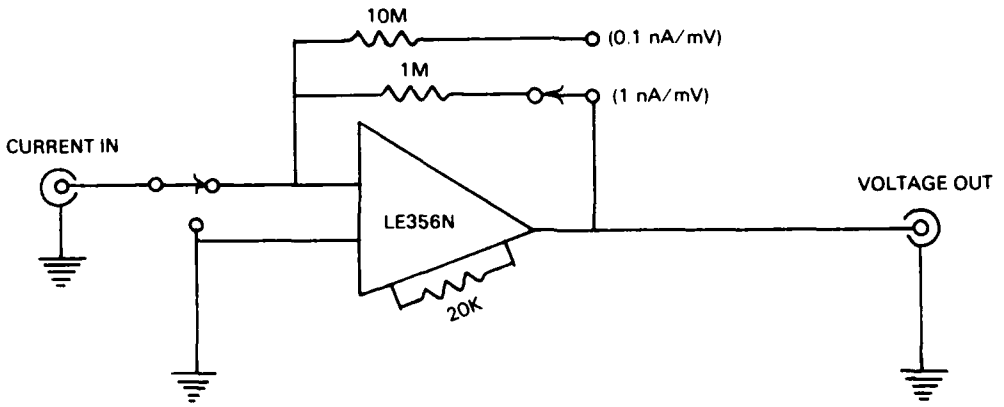

Figure 11. Current-to-voltage converter.

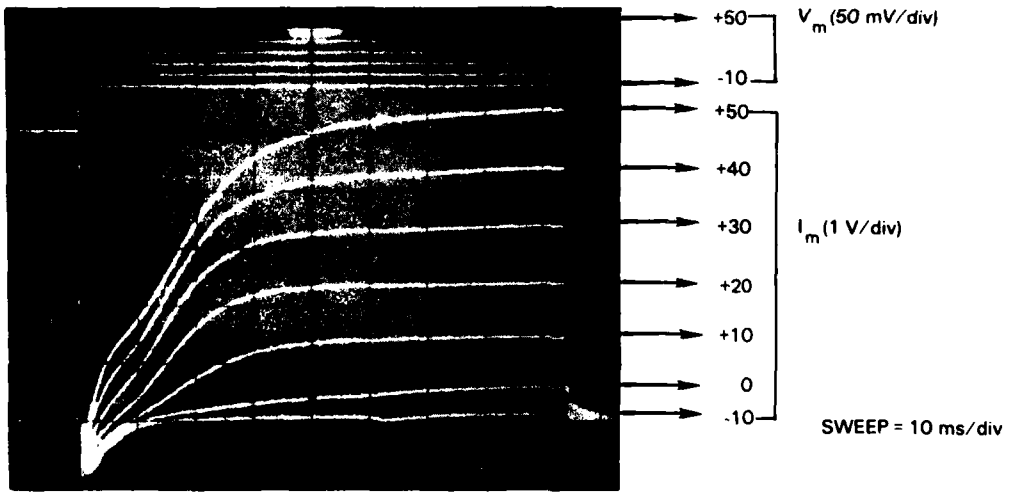

Figure 12. A clamp series.

membrane currents (I_m) in response to the voltage clamp at each pulse level. Current amplitudes were measured from the Polaroid prints for all experiments run before December 1983. After that date, currents were also digitized by a microprocessor system and stored on disk.

MICROPROCESSOR SYSTEM

Beginning in December 1983, a microprocessor was added to the experimental system. Data to be collected and stored in the microprocessor system included interspike interval (ISI), membrane current during a voltage clamp pulse (I_m), holding potential prior to a voltage-clamp pulse (V_h), potential of the command pulse, and membrane potential during a voltage-clamp pulse. The cell's resting membrane potential (V_m) was also determined and stored, and the condition of microwave exposure was coded.

The microprocessor consisted of a 24-slot STD bus card cage (MicroSys SBS0000) with a Z80 central processor card (Mostek MDX-CPU1), a floppy disk controller card (MicroSys SB8500), a serial interface card (MicroSys SB8420), a parallel interface card (MicroSys SB8466), and an A/D card (MicroSys SB8260). In addition, one wire-wrap card was used to incorporate data input and manipulation capability. The basic components of the wire-wrap card included counter time circuit (CTC), parallel I/O chip (PIO), JK flip-flops, Schmitt trigger, logic gates, multiplexer, switches, and operational amplifier. Peripherals to the microprocessor included two 8-inch disk drives, a terminal (Visual 200), a printer (Epson MX80), a video plotter (Tektronix 4012), and a hard-copy unit (Tektronix 4632).

Figure 13 shows the incoming data signals and the needed hardware routing in the microprocessor. The electrical activity of the cell (action potentials), as measured by the M-707 amplifier, was again amplified (by a Tektronix AM502) and used to trigger an event timer (CTC) via the Schmitt trigger and flip-flop. The events corresponded to action potentials, and the data from the timer were obtained by means of the ISI. The same data from the M-707 were amplified by a second Tektronix AM502 to yield a signal between ±5 V before being input to the A/D converter. This information was used to

determine resting V_m and to monitor V_m during voltage clamping. The current data were also amplified to the ±5-V range before being digitized and stored.

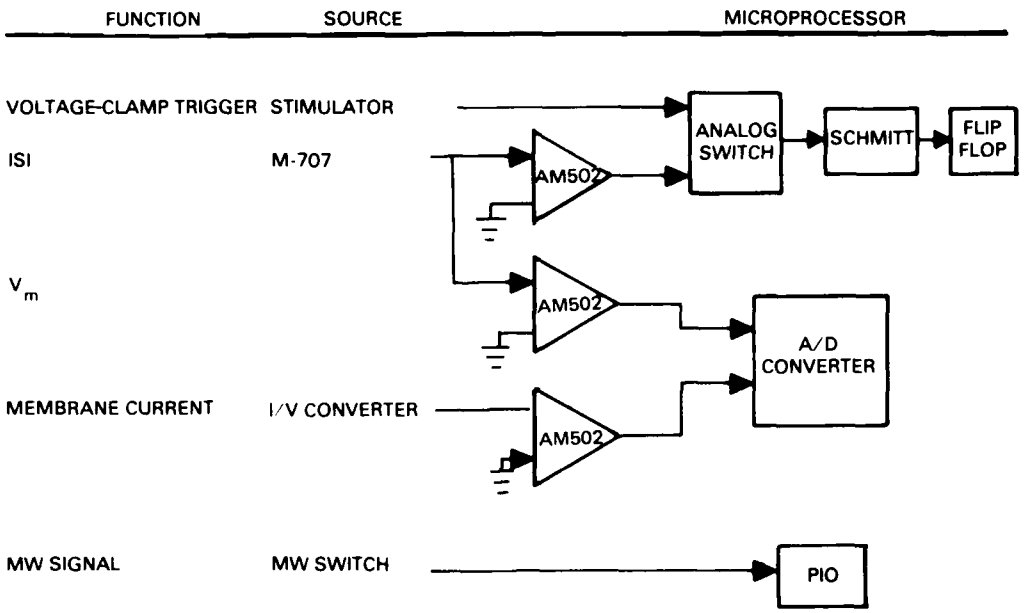

Figure 13. Routing of incoming data signals.

The microprocessor system was warned 10 ms prior to initiation of the command pulse to start collecting voltage-clamp data. A 3-V trigger from the stimulator was switched via an analog switch into the same flip-flop network used by the ISI signal. When the experimenter indicated by means of the terminal that a voltage-clamp series was to take place, the software monitored the output of the flip-flop to determine when the voltage clamp started. When the flip-flop was set, the microprocessor began digitizing and storing V_m and I_m. The trigger signal was generated by the stimulator when the experimenter pressed the pulse button. Delay circuitry inside the stimulator delayed the output of a pulse for 10 ms. Therefore, 10 ms of prepulse V_m and I_m baseline data were collected in addition to the data taken during the command pulse.

A circuit to deliver 5 V when a switch was closed was designed to indicate the switching in and out of the microwave energy. A microwave switch was

used to divert the microwave energy from a dummy load to the stripline containing the neuron being studied. When this switch was closed (diverting power to the stripline), a 5-V signal was sent to one bit of one channel of a PIO. The software then periodically monitored this PIO bit. When the bit changed state, a code was stored in memory to indicate the initiation/termination of exposure.

The software was written in MBASIC with specific hardware manipulations done by means of Z80 subroutines and disk access being done by means of CP/M commands. MBASIC then provided the program skeleton. The experimenter communicated with the program via MBASIC. On power up or reset, MBASIC queried the experimenter for name, date, and other pertinent facts related to the experiment. The experimenter then received options as to which program to run. The experimenter's options included: collect ISI data; display ISI analysis on printer or screen; determine membrane potential; display membrane potential; collect voltage-clamp data; display voltage-clamp data; and terminate data collection.

Analysis of ISI data included the display of the mean ISI, maximum ISI, minimum ISI, standard deviation, and number of ISIs counted. Histograms of the number of ISIs versus ISI interval were plotted on the Tektronix plotter. Hard copies of these histograms were obtained. Figure 14 is a tracing of one such histogram.

A time course of the digitized V_m and I_m collected during a voltage-clamp series could also be displayed on the Tektronix plotter. Figure 15 is a tracing of a hard copy of one of these plots.

After an experiment was completed, the software allowed access to the stored data, and a printer output summary of the data collected could be obtained. Figure 16 shows a sample summary. In addition, plots of outward current (at selected times into the clamp pulse) versus time for any or all pulse levels could be constructed on the video plotter (or other compatible plotter) and hard copies obtained. Figure 17 is a sample of this type of plot.

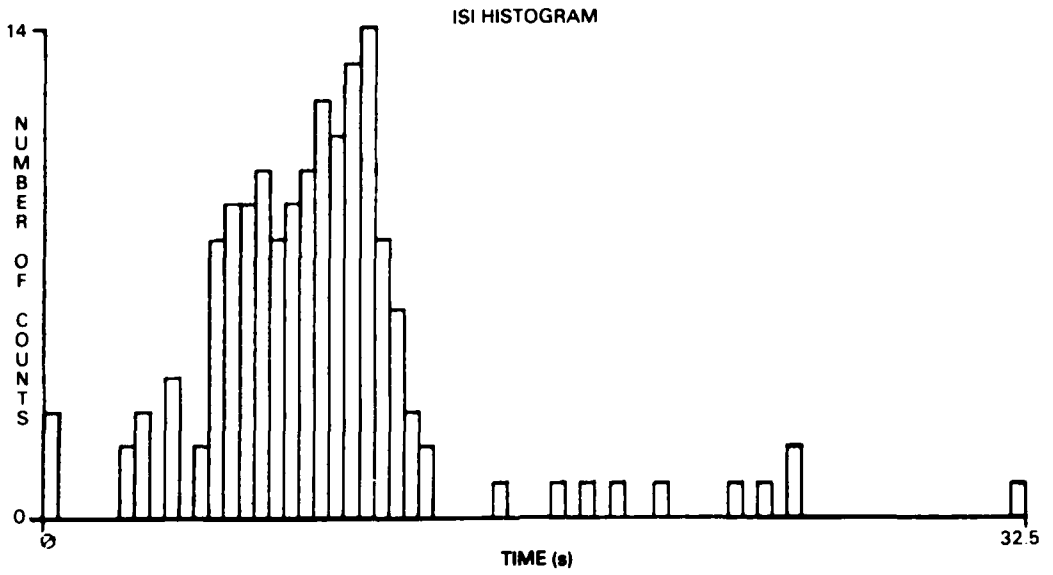

Figure 14. Interspike interval histogram.

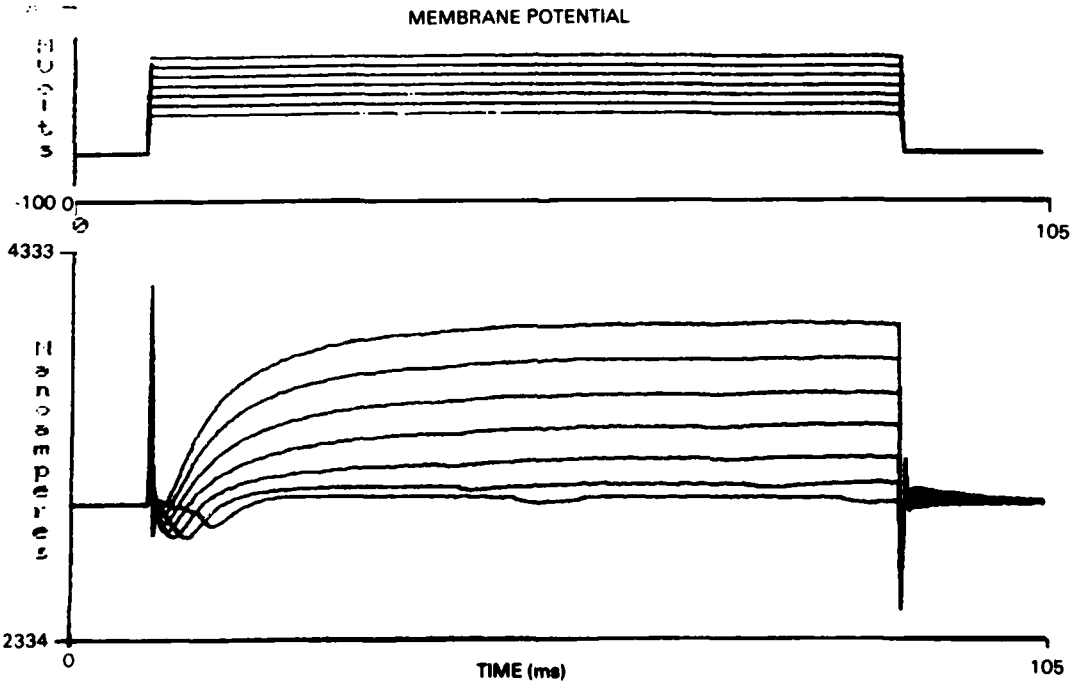

Figure 15. Video display of digitized I_m and V_m.

EXPERIMENTER	DATE	TIME	FILE
NLE	SEPTEMBER 12 1984	1255	SEP12VPN

ITEM	TIME	MW	DATA DESCRIPTION					
1	5 1	OFF	MP[1]	38 818				
2	5 5	OFF	VC[2]	20 012	20 024	-50 228	-1881 350	1570.800
3	5 9	OFF	VC	24 048	29 482	-49 984	-1461 430	2271.480
4	6 1	OFF	VC	28 394	39 404	-49 788	-1041.500	2972 170
5	6 4	OFF	VC	32 686	49 243	-50 326	-602.051	3724 120
6	19	OFF	MP	-50 293				
7	19 5	OFF	ISI[3]	0 563	19 621	10 484	4 147	30
8	19 6	OFF	MP	-39 014				
9	19 9	OFF	VC	21 292	23 018	-47 298	-1686.040	1678.220
10	20 3	OFF	VC	25 388	32 485	-47 266	-1322.270	2352.050
11	20 5	OFF	VC	29 773	42 617	-47 559	-943.848	3074.710
12	20 8	OFF	VC	33 816	51 953	-47 380	-550.781	3807.130
13	33 4	OFF	ISI	0 629	55 305	12 586	13 071	53
14	34 2	OFF	MP	-41 797				
15	34 6	OFF	VC	21 702	23 823	-45 882	-1827.640	1741.700
16	35 2	OFF	VC	25 916	33 545	-46 517	-1407 710	2444.820
17	35 5	OFF	VC	29 822	42 739	-46 322	-995.117	3182.130
18	35 7	OFF	VC	34 231	52 896	-46 029	-514.160	3946.290
19	48 9	OFF	ISI	0 578	15 441	5 031	3.542	144
20	50 5	OFF	MP	-58 008				
21	50 9	OFF	VC	21 614	23 667	-46 729	-1598.140	1775.880
22	51 4	OFF	VC	25 632	33 003	-46 615	-1246.580	2488.770
23	51 6	OFF	VC	30 034	43 105	-46 631	-831.543	3211.430
24	51 9	OFF	VC	34 163	52 642	-46 403	-392.090	3929.200
25	57 9	OFF	ISI	52 082	132 775	92 429	57.059	2
26	65 2	OFF	ISI	0 611	18 217	10 294	3 452	41
27	65 8	OFF	MP	-43 848				

1 MP is membrane potential in mV

2 VC is voltage-clamp data in following order

COMMAND VOLTAGE (mV)	PULSE LEVEL (mV)	HOLDING POTENTIAL (mV)	INWARD CURRENT (nA)	OUTWARD CURRENT (nA) AT 80 ms

3 ISI is interspike interval in following order

MINIMUM ISI (s)	MAXIMUM ISI (s)	MEAN ISI (s)	STD DEV OF MEAN	NUMBER ISI COUNTED

Figure 16. Sample of data summary.

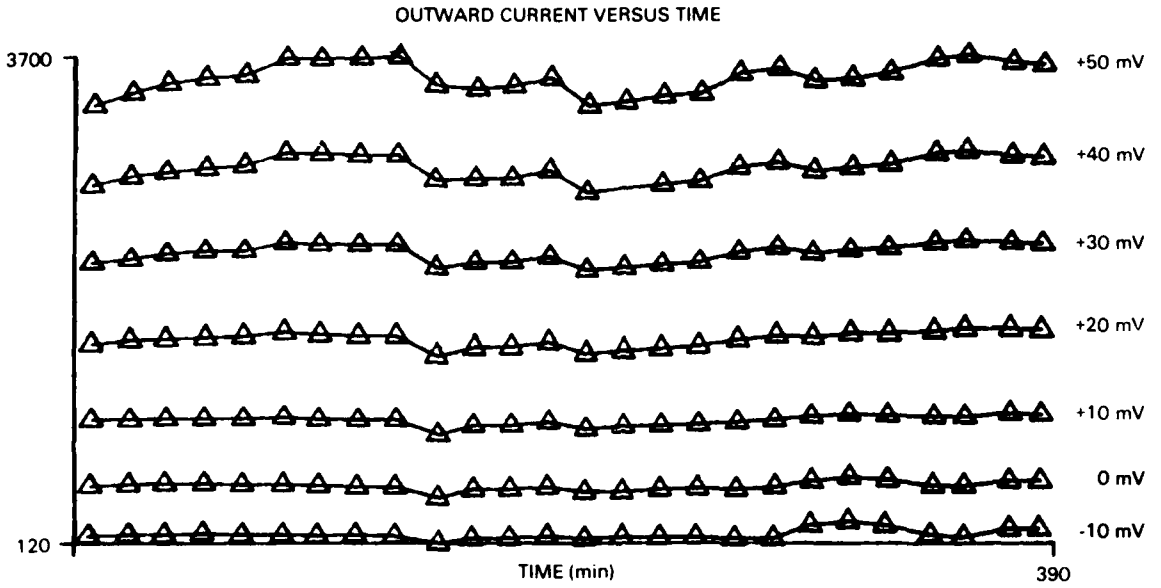

Figure. 17. Plot of digitized outward current versus time.

MICROWAVE EXPOSURE EQUIPMENT

Both a low-power and a high-power source were used to generate the 2.45-GHz microwave signal. Figure 18 is a block diagram of these two sources and how they were connected to the stripline. The low-power source was the one used in the previous firing frequency study, and is described in detail in TR 698 (Campbell and Brandt, 1982).

The high-power source consisted of a Gerling-Moore Variable (up to 2 kW) Microwave Power System (Control Unit Model 4006 and Power Source Model 4003; Thermex, Palo Alto, CA). The output of the power source fed a waveguide terminating in a waveguide-to-coaxial converter. The coaxial coupling fed the signal via cable to a directional coupler mounted on the stripline fixture. A -20-dB attenuator was connected between the thermistor mount and the directional coupler to reduce the power to a level suitable for the HP431B power meter, resulting in a total attenuation of 40 dB. For the use of this source, a high-capacity 50-ohm load was attached via coaxial cable to the termination of the

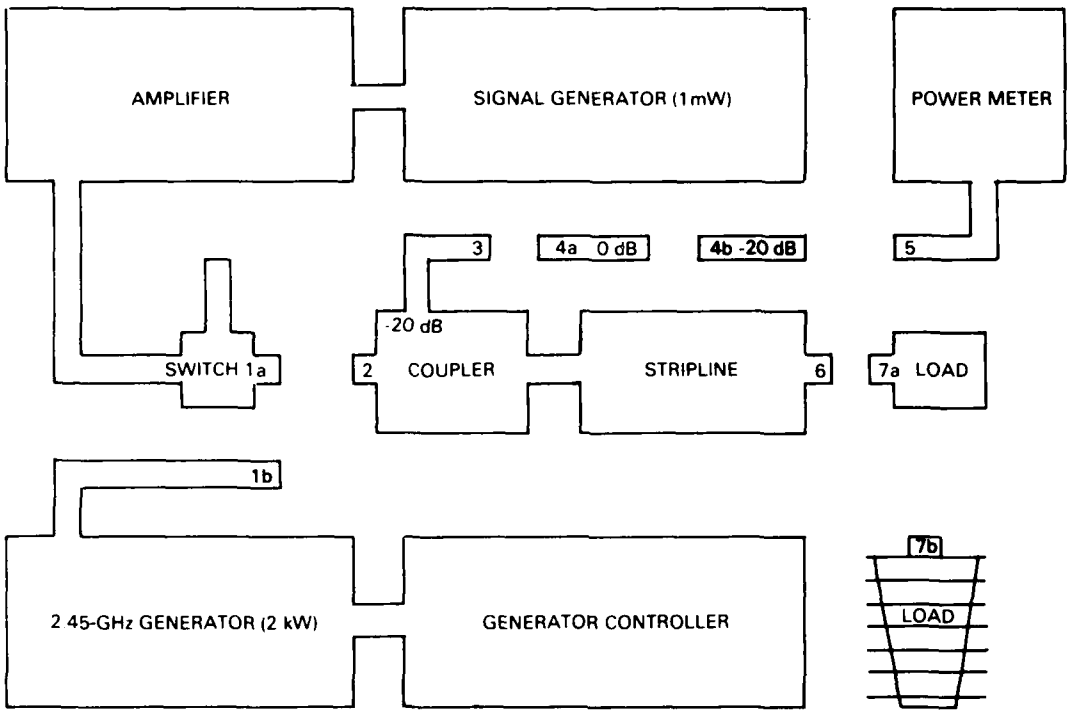

Figure 18. Block diagram of microwave exposure experiment.

stripline, replacing the small-capacity load used with the low-power source. The high-power source was not operated above an incident power of 8 W in any of the experiments. In some experiments, a coaxial switch was incorporated to direct energy to a load or to the stripline.

SPECIFICATION OF EXPOSURE

To compare the results of different experiments, the microwave exposure must be specified precisely. One way to do this is to indicate the power density (mW/cm^2) in the stripline and the duration (s) of the exposure. The product of these terms is the exposure dose and is measured in the units $mJoules/cm^2$. However, this exposure does not indicate how much energy is actually absorbed by the tissue. A more desirable way to express the exposure is in terms of the specific absorption rate (SAR). SAR is defined as the power absorbed per gram of tissue and has units of mW/g or W/kg.

SAR can be determined directly or indirectly. In a direct determination, the power transmitted through but not absorbed by the sample is measured (P_B) and subtracted from the power incident on the sample (P_A), as shown below.

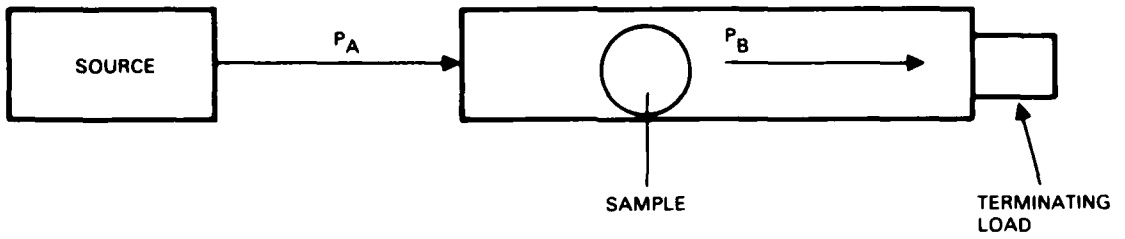

The result should be the power absorbed by the sample (P_S), assuming that no energy is reflected back from the load:

$$P_A - P_B = P_S \quad .$$

The calculated absorbed power, P_S, is divided by the mass of the sample to yield mW/g. In our system, the mass of the nervous tissue is so small that the amount of energy absorbed cannot be determined by this method.

Allis, et al. (1977) described an indirect method for determining the SAR. In this method, the tissue is replaced by a material of similar specific heat, generally water, and the change in temperature of the material is determined during and following microwave exposure. From either the heating or cooling curves, the SAR may be calculated. A limitation of this method is a requirement that temperature changes of 2.5°C or larger are required for accuracy. Since most of our work was done with the low-power source, which produced temperature changes much less than 0.5°C, we could not measure SAR by this method either. However, as soon as the high-power source went into service, we could determine the SAR at various power levels.

Figure 19 is the temperature profile of 0.140 ml of sea water in the ganglion chamber exposed to 4.65-W incident power. Temperature was monitored by a thermocouple placed in the center of the water in the ganglion chamber. The symbols on the curve define the parameters measured in order to calculate the cooling constant, k, from the formula

$$\ln\Delta T = -k(t - \tau) + \ln\Delta T_{\tau}$$

where

T_o = initial temperature of the system

ΔT_{τ} = temperature reached at termination of exposure

T = temperature reached at time t

$\Delta T = T - T_o$.

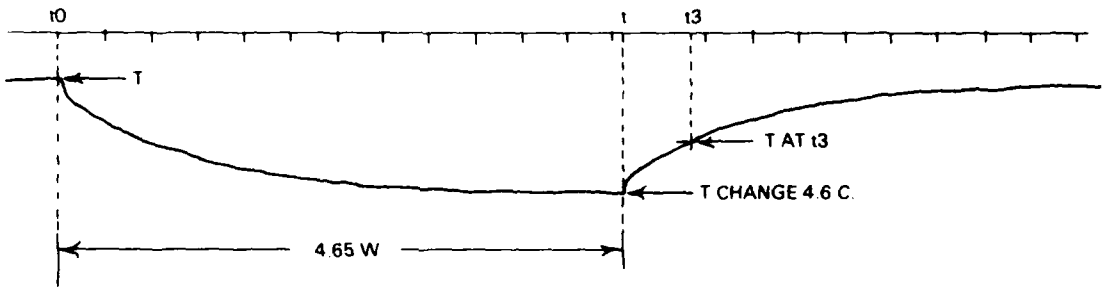

Figure 19. Temperature (T) profile and cooling curve.

Table 1 gives measured and calculated values for 10-second time periods measured on the cooling curve in figure 19. A plot of $\ln\Delta T$ versus time yields a straight line whose slope is $-k(s^{-1})$, in this case 0.0113 s^{-1}.

Table 1. Temperature calculations from data of figure 19.

$t - \tau$ (s)	ΔT (°C)	$\ln\Delta T$
10	3.85	1.35
20	3.20	1.16
30	2.75	1.01
40	2.45	0.90
50	2.00	0.69
60	1.70	0.53
70	1.50	0.41
80	1.30	0.26
90	1.10	0.10
100	0.90	-0.11
110	0.80	-0.22
120	0.70	-0.36

SAR is calculated from the equation

$$SAR = C * k * \ln\Delta T_{\tau}$$

where

C = specific heat of sea water, 3.91 J/g

k = cooling constant

ΔT_{τ} = temperature reached at the termination of the microwave exposure.

Figure 20 is a plot of SAR values determined in three separate experiments for different values of incident power. In these experiments, the initial temperature of the system was 10°C. The line connecting the points is fitted by eye.

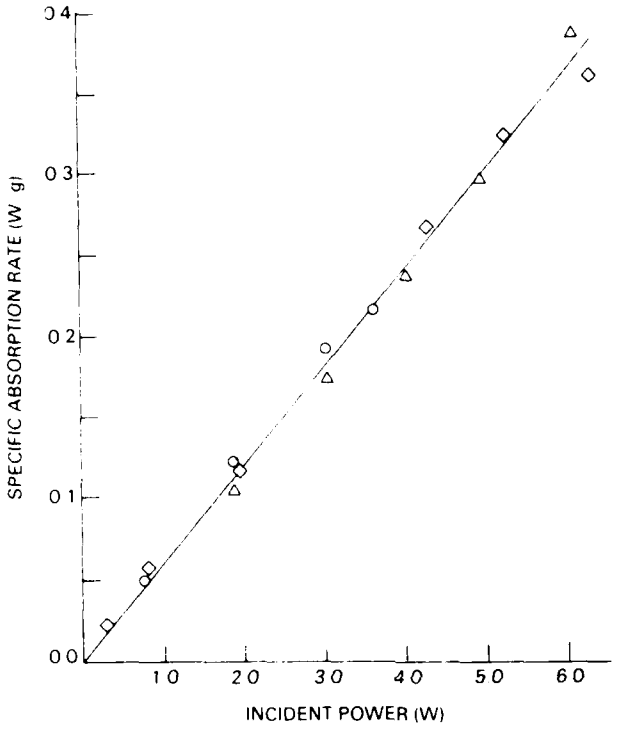

Figure 20. Specific absorption rate versus incident power.

Questions arise in utilizing the SAR values determined in this manner. During an experiment with nerve cells, two microelectrodes penetrating a neuron are present in the stripline and sea water is flowing through the chamber. How do these differences influence the SAR?

A number of experiments were run to measure the effect of electrodes and sea-water flow on the microwave-induced temperature change. Figure 21 plots the temperature reached at termination of microwave exposure (ΔT_τ) versus incident microwave power for different exposure conditions. These exposure conditions include: (1) no flow, no electrodes (condition during SAR measurement discussed above); (2) no flow, two electrodes; (3) low flow, two electrodes; and (4) high flow, two electrodes. As observed from these plots, the presence

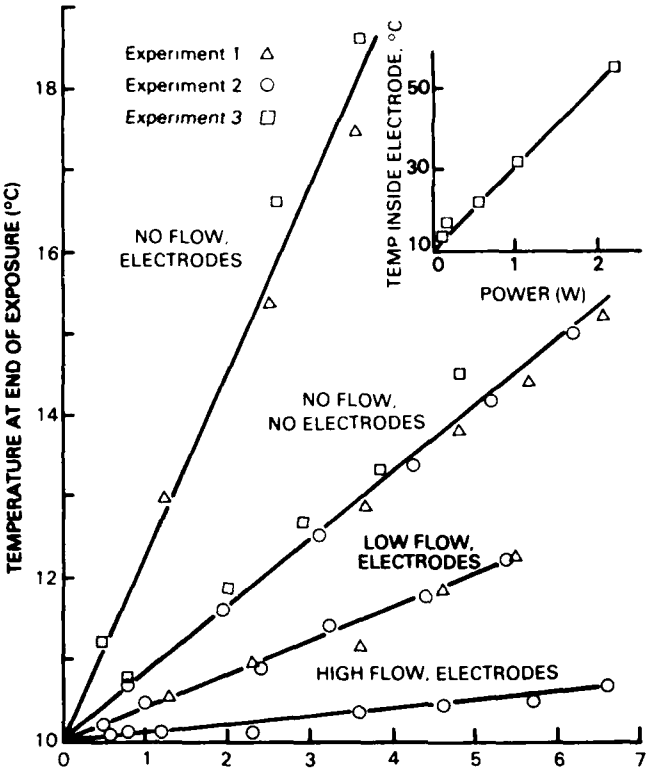

Figure 21. Temperature at end of exposure versus incident power.

of the two microelectrodes in a stationary volume of sea water caused a temperature change almost triple that produced in the sea water alone. This dramatic increase in microwave-induced temperature change may have resulted from heat transfer from the microelectrodes into the sea water. The inset plot in figure 21 shows the temperature recorded from a thermocouple inserted into a KCl-filled microelectrode that was placed inside the stripline during exposure. An exposure of 2 W raised the microelectrode temperature 40 degrees above the ambient within a few seconds. Apparently, then, microwave energy heats the electrodes, and because the heat generated in the electrodes is much greater than that generated in the sea water, heat is passively transferred from the electrodes into the sea water. Thus the sea water is heated by two methods: direct microwave heating and indirect conductive heating. This information demonstrates the need for adequate cooling of the ganglion environment

to prevent thermal effects, even at SARs believed to produce no temperature change in the ganglion.

The total temperature change in the sea water is reduced by flowing cooled sea water through the chamber--the higher the flow rate, the lower the temperature change (fig 21). These data prove the success of a flow system in minimizing heating of the ganglion. The flow system even obviates the added heating from the electrodes.

Since the electrodes provide a second heat source, the method to determine SAR by the temperature change induced by microwave exposure could not be used when the electrodes were present. The SARs calculated from the no-flow, no-electrode measurements were considered good approximations to the electrode flow condition and, therefore, were used to describe absorption by the ganglion. The tissue is stationary, held by cactus spines during the exposure, and thus is comparable to the stationary sea water. The flowing sea water may remove heat produced in the tissue by microwave exposure, but will not alter how much energy is absorbed. SAR values reported in the results are therefore based on the plot in figure 20. Since most of our exposures were below an incident power of 1 W, the SAR values given for those experiments were determined by extrapolation on the plot in figure 20.

INTERPRETATION OF IONIC CURRENT

The major components of the current observed when an Aplysia neuron is voltage clamped were indicated in figure 5. A number of factors can influence each of these components and, in turn, complicate the interpretation of the current trace. Ideally, the voltage clamp should be designed and operated to minimize the complicating factors. Already described are how the gain and voltage output of the differential amplifier were designed to produce a fast rise time and to hold the V_m at the desired value without ringing (see Differential Amplifier and Current Gain, above). Ringing was also reduced by using low resistance (0.6 to 1.2 MΩ) electrodes (see Microelectrode Preparation, above). Described below are other factors that can confound the interpretation of the membrane current trace.

The capacitive current results from the discharge of the membrane's intrinsic capacitance when the membrane is depolarized. The magnitude of this current is dependent on the amount of depolarization and typically settles in a time much less than 1 ms. However, in practice, other capacitances can add to the membrane capacitance and greatly increase the settling time of this current. External capacitance (capacitance not associated with the membrane) was minimized by careful placement of the electrodes with respect to each other, the suffusion channels, and the stripline. Some of the external capacitance was neutralized by the capacity compensation capability in the M-707s.

Another factor complicating the interpretation of the membrane currents is the presence of glitches, periodic inward currents appearing on the outward current tracing. Figure 22a shows current traces with multiple glitches. These inward currents result when the voltage-clamp current is insufficient to hold the soma and axon membrane at the same potential. This is called an inadequate space clamp. Apparently, the axon membrane, rather than being held at a steady depolarized potential, can recover from the initial depolarization, generate an action potential, recover, generate another action potential, etc. The voltage-clamp circuitry reacts to the inward currents accompanying each action potential, resulting in the glitches. While this explanation of glitches seems reasonable, supporting evidence was desirable. Figure 22b shows that perfusion of a clamped cell with Na^+-free artificial sea water eliminates the glitches, thus demonstrating that they result from transient increases in Na^+ conductance. In most instances, cells showing glitches were not analyzed. In the few cases in which data demonstrating glitches were analyzed, the glitches were ignored.

ANALYSIS OF DATA

At the outset of this research, it was decided that peak inward and peak outward currents would be digitized for analysis. These data would provide information on (1) voltage-dependent early inward Na^+ current and (2) voltage-dependent late outward K^+ current. In addition, changes in the current waveform would be looked for in order to spot microwave influences on other membrane currents; for example, the late inward Ca^{++} current. Changes during microwave exposure in the peak inward or outward currents, or in the current

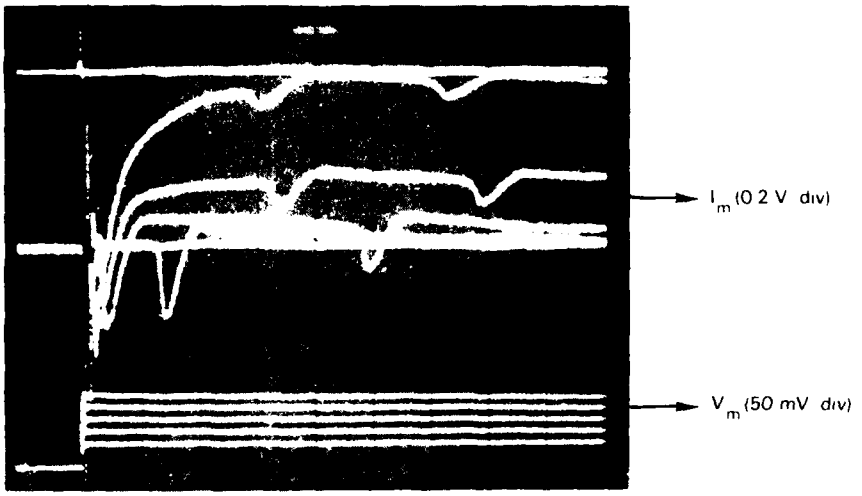

a In sea water

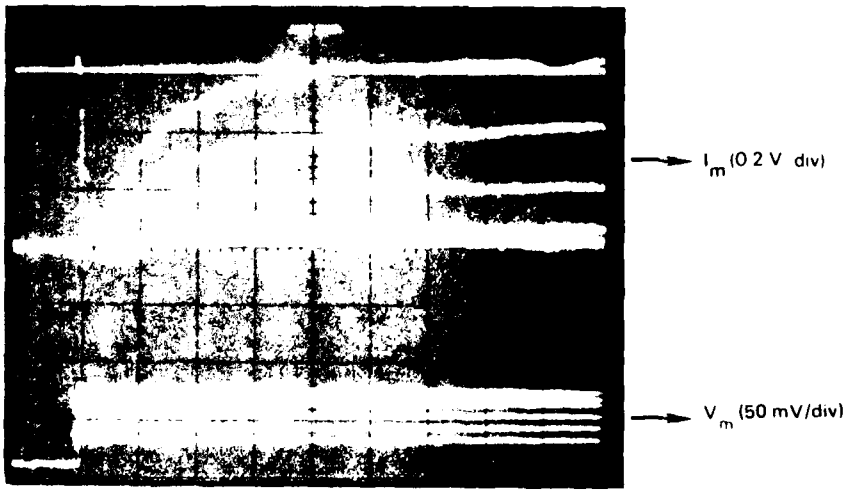

b In Na^+ free artificial sea water

Figure 22. Glitches are Na^+ currents

waveform, would indicate a microwave influence on membrane channels. The specific channel(s) being affected could be determined by either selective channel blocking or selective ion depletion in the sea water.

As the research continued, it became apparent that measurements of the peak early inward current were erroneous because of ringing and/or superimposed capacitive currents. Therefore, only the late outward current and the overall voltage waveform were examined.

The outward current magnitude was measured initially at 40 ms after initiation of the depolarizing pulse, but in most later experiments it was measured at 80 ms. The outward current was generally stable at 80 ms, or increasing or decreasing only slightly, so measurements at this time provided a good measure of the peak current. This time frame has been used by others as a measure of outward current; see, for example, Thompson (1977).

Measurement of outward current magnitude was made on the Polaroid photographs of the oscilloscope screen displaying the current traces in storage mode. The resolution of this measurement was limited to 0.25 mm on the photograph. Since the current-to-voltage monitor output was 1 mV per 1 nA, a 0.25-mm resolution could represent 5 nA (at an oscilloscope sensitivity of 0.1 V per division) to 100 nA (at an oscilloscope sensitivity of 2 V per division). Most outward currents were in the range of 2.5 to 6.0 μA, so the oscilloscope sensitivity was set at 0.5 or 1 V per division. The resolution of the Polaroid film measurements was, therefore, between 25 and 50 nA. When the microprocessor became available, the resolution of the measurement of outward currents was increased to 4 nA.

Since each clamp series consisted of the current elicited by each of seven different depolarizing pulses, plots of the outward current at 80 ms versus the membrane potential (during the clamp pulse) were constructed from each series. Figure 23 is an example of such a plot.

Preliminary results plotted this way suggested that microwave-induced changes in conductance would be most conspicuous at the highest pulse levels (+50 mV). Accordingly, time course plots of the outward current at 80 ms for the +50-mV pulse were made of each experiment. Figure 24 shows examples of such a plot.

EXPERIMENTAL PROTOCOL

The experimental protocol varied during the early development period of this study. In early experiments, the holding potential used was that of the cell's resting membrane potential, resulting in different holding potentials for different cells and, on occasion, holding potentials that changed during an experiment (as the cell's membrane potential changed). The reasoning behind this choice was to hold the cell such that zero net current would pass across the membrane. By early 1983, however, a fixed holding potential of -50 mV was chosen to standardize all cells. This potential was chosen because it was near the reported membrane potential of most Aplysia neurons (Kandel, 1976) and, more importantly, because it held the channels carrying the early outward potassium current in an inactivated state, thus removing the current from consideration in the current traces.

Pulse levels in early experiments were recorded to membrane potentials of -20 to +35 mV. In early 1983, the pulse levels were standardized to boost the cell from a holding potential of -50 mV to -10, 0, +10, +20, +30, +40, and +50 mV. The pulse sequence was always from the more negative potential to the more positive potential (i.e., -10 to +50 mV), with a consistent 15-second pause between pulses to each different level.

In a few experiments, prepulses to -90 mV were delivered for 30 ms just prior to the depolarizing pulse. These experiments were attempted to improve the appearance of the inward currents, by ensuring the activation of the Na^+ channels so that they could be opened during a voltage pulse. (The voltage-dependent Na^+ channels opened by a depolarizing pulse close after 1 ms in an

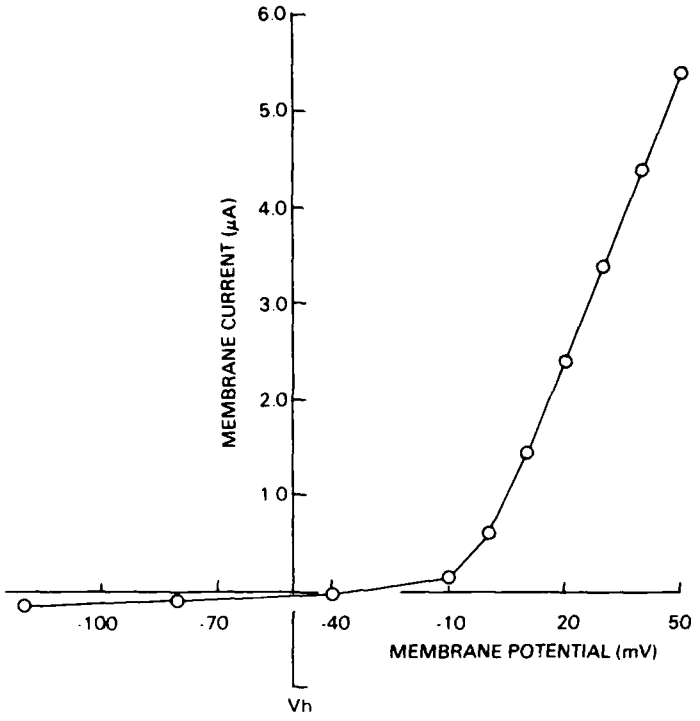

Figure 23. Membrane current versus membrane potential.

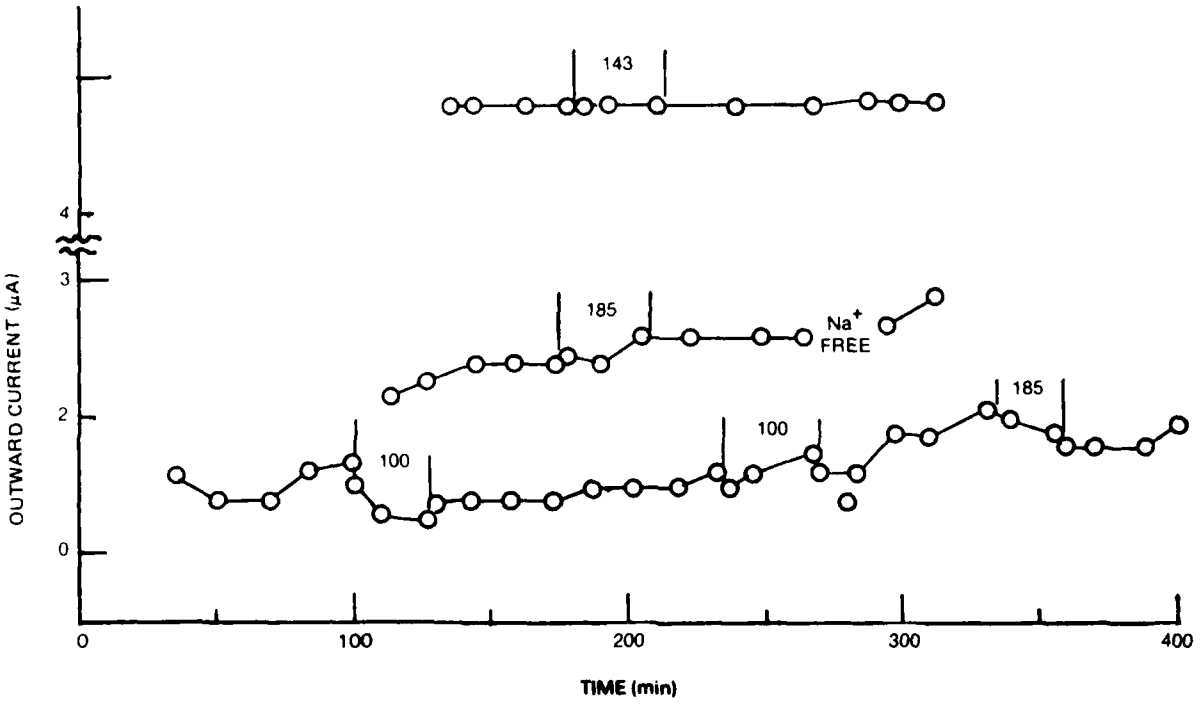

Figure 24. Time course plots of peak outward current during 50-mV clamp pulse.

inactivated state. A hyperpolarization to nearly -90 mV is required to activate them so that they may again be opened by a depolarization.) However, the prepulse did not produce the desired improvement of inward currents, and was discontinued.

In general, the period between clamp series was consistent throughout the study. Figure 25 shows a typical protocol with regard to time. The time at which the cell became successfully impaled with two microelectrodes was called time zero (T_0). The first 30 to 90 minutes of the experiment consisted of a waiting period during which the cell's recovery from impalement was monitored. During this period, the cell's membrane potential usually increased, and often a pattern of spiking was established. On most occasions during this recovery period, the cell was pulsed with constant current pulses (see Cell Impalement and Signal Monitoring, above).

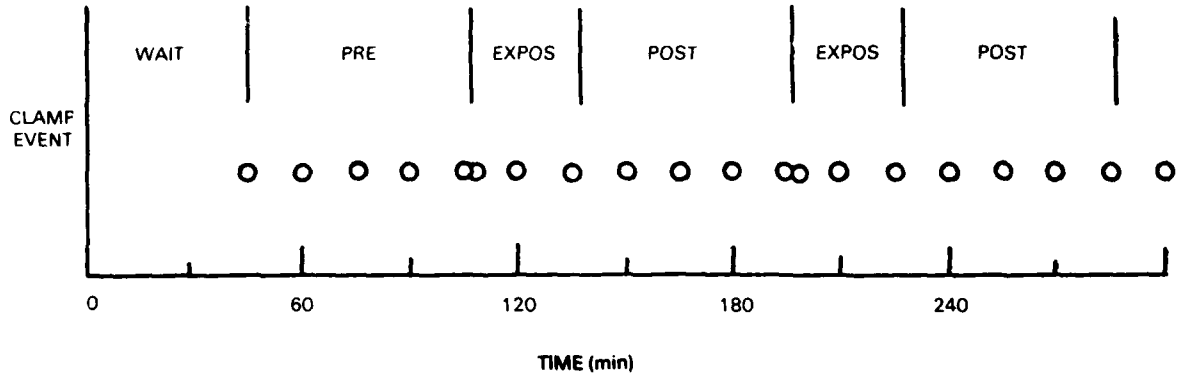

Figure 25. Experimental protocol.

Following the waiting period was a pre-exposure period, during which four or five clamp series were performed at 15-minute intervals. This period served to provide a baseline for currents, which were expected to reach some

stable level during this period. There then followed a period during which the cell was exposed to microwave energy: the exposure period. Clamp series were sometimes taken immediately after onset and termination of the microwaves, as indicated in figure 25. This practice was discontinued when it appeared that clamp series done within 2 minutes of a previous series always yielded lower current levels. The exposure period was routinely 30 minutes and was followed by a post-exposure period of 45 to 60 minutes, during which clamp series were performed every 15 minutes. If the cell was still functioning well after this post-exposure period, another exposure was given, followed by a second post-exposure period.

RESULTS

The first 6 months of this project were occupied with constructing and testing the voltage-clamp apparatus. Another 6 months were devoted to acquiring skill in the use of the apparatus and in interpreting the current traces obtained. Experiments to ascertain the possible effects of microwave exposure on the neuron membrane currents were begun in June 1982.

A certain amount of subjectivity was involved in determining the experimental characteristics required to define the data as natural (not influenced by experimental problems) and worthy of analysis. As experience was gained doing experiments, and as current traces were compared with published data, the subjectivity in experiment selection diminished. Thus, aided by hindsight, we judged those experiments performed in the early part of 1982 as inadequate. Only those experiments since September 1982 were analyzed and will be discussed.

A total of 105 cells were studied, 34 of which were exposed to 2.45-GHz energy. The breakdown as to cell type (beat, burst, silent), as well as specific cell identification, are shown in tables 2 and 3. Because of the large number of experiments performed in this study, much data were available on

membrane currents under conditions other than microwave exposure. Therefore, interpretation of nonmicrowave influences will be included in the analysis.

MEMBRANE CURRENTS AS A FUNCTION OF TIME

During the long period (greater than 2 hours) required for an exposure experiment, variables other than microwave exposure (temperature, ion concentration, pipette displacement, reference electrode potential, and microelectrode tip potential) can influence the magnitude of the outward current. Even in the absence of these artifactual conditions, the cell may have inherent current changes over time. These inherent changes must be considered when analyzing the membrane currents for microwave effects.

Plots of outward current for a +50-mV pulse measured at 80 ms versus elapsed time provide information on the stability of membrane currents. Figures 26, 27, and 28 are such plots for beating, bursting, and silent cells. The plots are presented for the different cell activities in order to observe potential characteristic changes over time of the different cell types. Some microwave exposures are also indicated on the plots to allow subjective comparison of inherent current variations over time with current variations during exposure. Only experiments lasting 200 minutes or longer, in which no other current-influencing variables had been identified, are plotted in these figures. The downward arrows signify the onset of microwave exposure, and the upward arrows signify the termination of exposure. SARs given at the end of the time course plots are in chronological order.

The time course plots indicate that there is some inherent variability in membrane current over time. The types of variation were similar for all three cell types, indicating no type-dependent characteristic changes over time; i.e., the firing pattern does not dictate the time variation in late outward current. These data also show that exposure to microwave energy in the SAR range of 20 to 36 mW/g produced no apparent change in late outward current that was consistent over the cells exposed, and that exceeded the inherent changes over time.

Table 2. Activity of cells studied.

	Total	Control	Exposed
Beat	28	20	8
Burst	41	30	11
Silent	36	21	15
Totals	105	71	34

Table 3. Identification of cells studied.

	Type	Control	Exposed
L1	1	0	1
L2	3	3	0
L3	10	4	6
L4	4	4	0
L5	3	2	1
L6	5	2	3
L10	1	0	1
L11	2	1	1
L13	4	2	2
R9	1	0	1
R11	1	1	0
R13	1	1	0
R15	4	3	1
VPN	5	3	2
Unknown	60	45	15
Totals	105	71	34

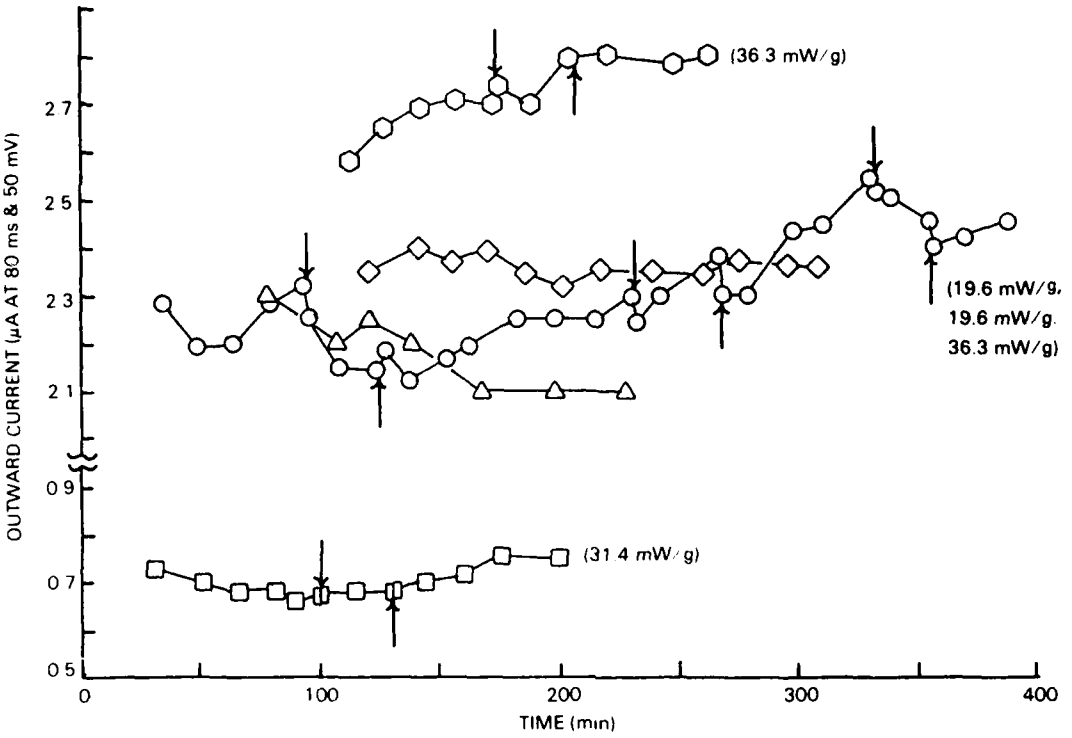

Figure 26. Time course plot of beaters.

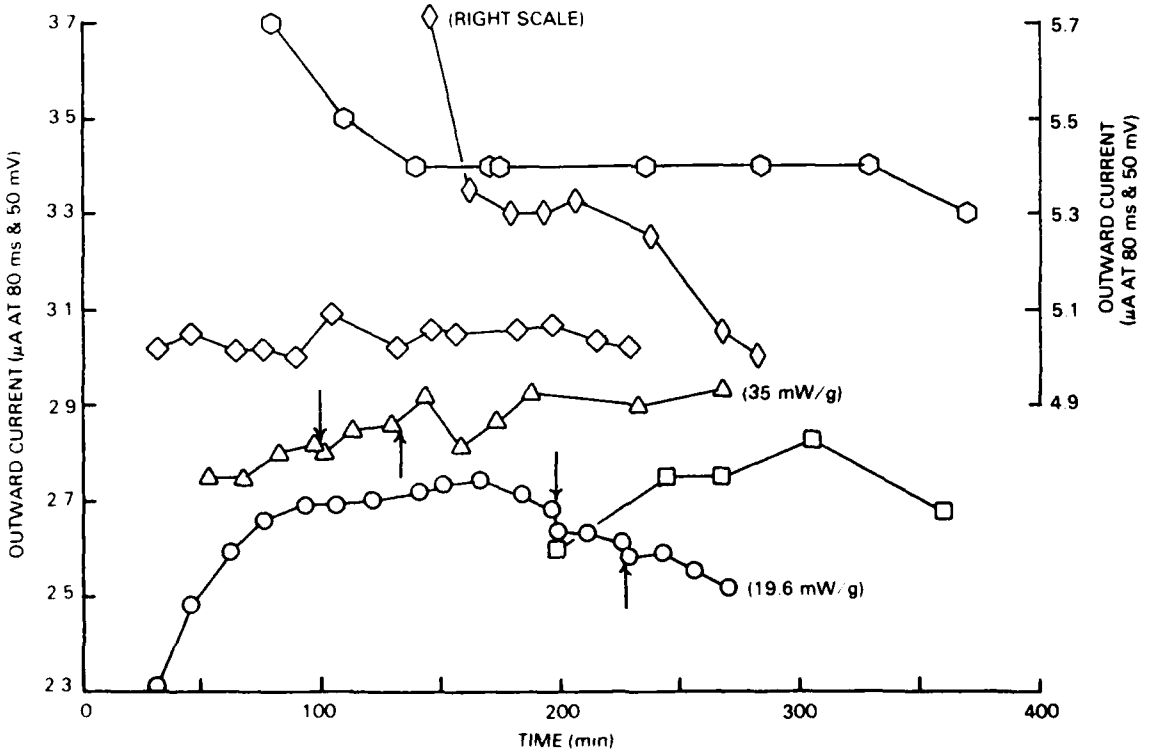

Figure 27 Time course plot of bursters.

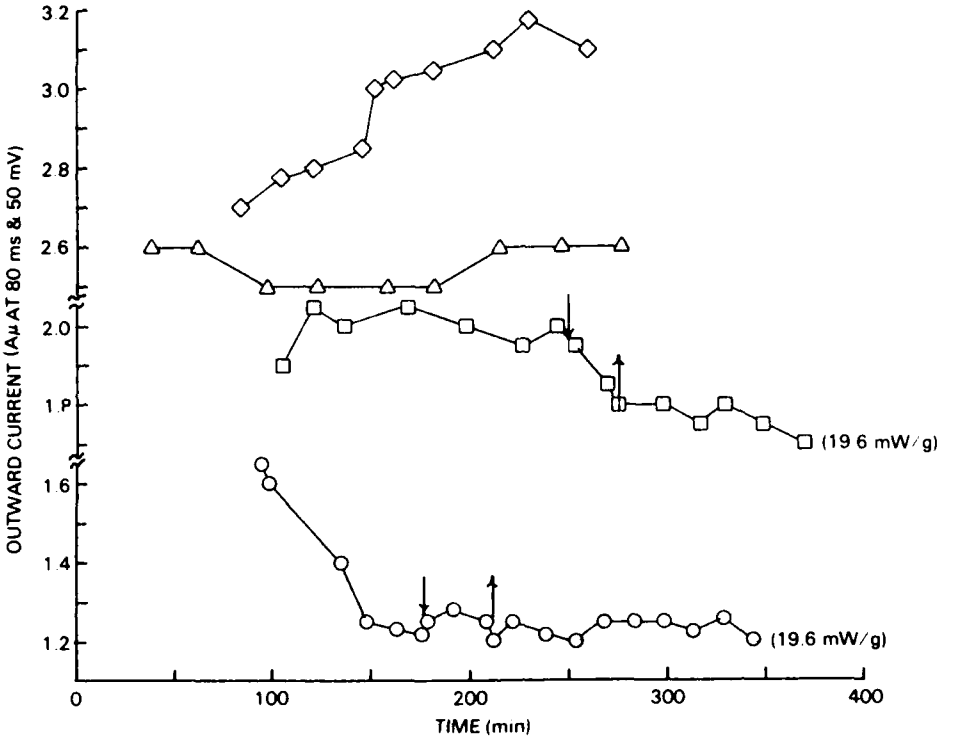

Figure 28. Time course plot for silent cells.

INFLUENCE OF CELL TYPE ON MEMBRANE CURRENT

Since the firing pattern of a cell is determined by the time course of the major ionic currents through its membrane (Conner and Stevens, 1971), cells with similar firing patterns should show similar ionic currents. Examination of the ionic currents of cells in our study revealed that the pattern of currents for the three cell types were distinguishable. Figure 29 shows representative examples of the three basic patterns. For the beating cell (Figure 29a), there is a fast inward current, followed by a smooth, rapidly rising outward current that plateaus and then tends to decrease as long as the depolarization is applied. In contrast, the bursting cell (figure 29b) shows a somewhat slower and larger inward current followed by a more slowly rising outward current, which indicates a slight depression at 8 to 10 ms, giving the curve something of an s-shape. This outward current does not plateau but, following the initial rise, continues to increase as long as the depolarization persists. The silent cells (figure 29c) are characterized by a very small inward current relative to the other two types. The outward current has a slight s-shaped

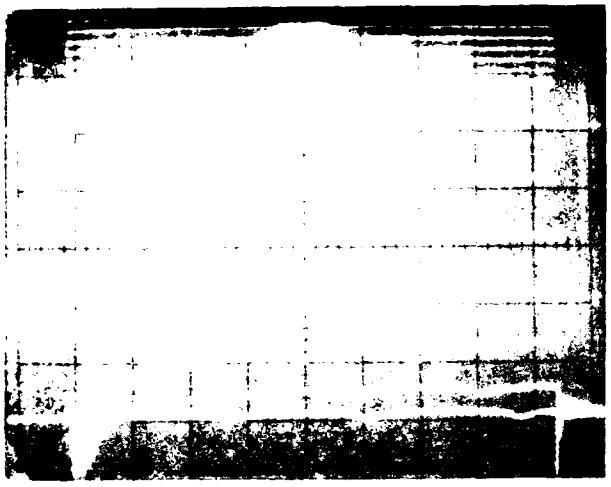

a. BEATER (VPN)

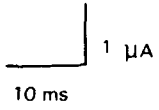

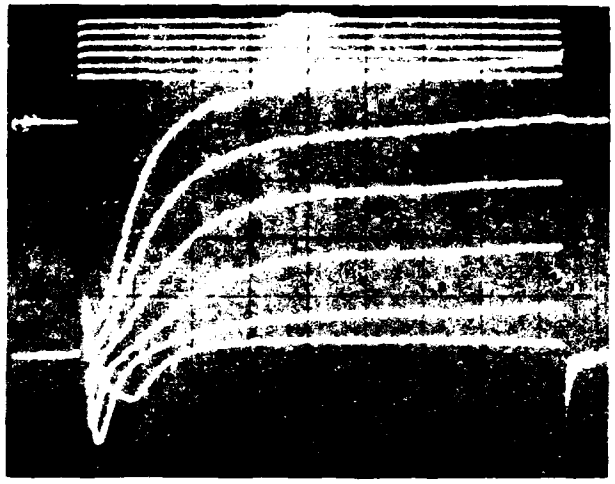

b. BURSTER (R15)

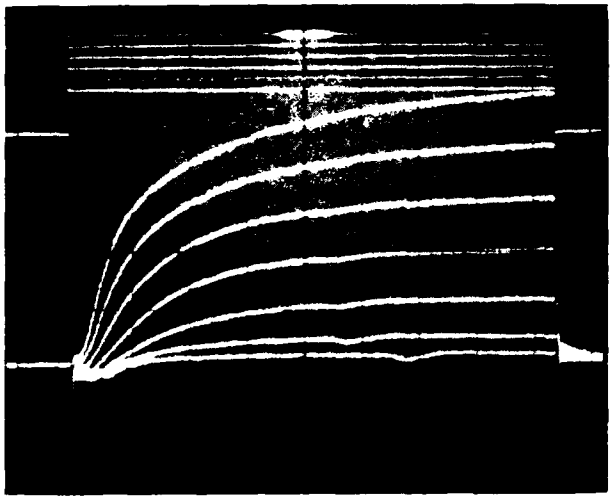

c. SILENT (L1)

Figure 29. Comparison of the shape of current traces for beaters, bursters, and silent cells at 15°C.

waveform rising somewhat more slowly than the burster. This outward current also does not plateau, but continues to increase while the depolarization lasts. These characteristic current patterns, therefore, support the theory that an alteration in firing pattern may result from an alteration in membrane currents.

EXPERIMENTS WITH THE VENTRAL PHOTORESPONSIVE NEURON (VPN)

Several experiments were performed by means of VPN because of its documented sensitivity to the light frequencies of electromagnetic energy (Andresen and Brown, 1979). The VPN hyperpolarizes in response to light and offers the opportunity to compare the effects of visible light and microwave exposure on outward membrane currents. In addition, the beating behavior of the cell permitted us to determine whether the effect of light on the ISI was similar to or different from the effect of microwaves. Two of the 10 experiments done with this cell are particularly interesting and will be described.

In one experiment, the effect of microwave exposure, temperature change, and visible light exposure on the ISI was determined with a single pipette in the cell. A second pipette was then inserted and the effect of the same variables on the outward membrane current determined. Figure 30 is a plot of the average ISI versus time for the experiment. The second pipette was inserted at 235 minutes into the experiment. The temperature control unit maintained a base temperature of 14.9°C. At 100 minutes, the cell was exposed to an SAR of 362 mW/g. During this exposure, the temperature within the ganglion chamber increased to 16.1°C. Concommitant with the microwave exposure and temperature change, the ISI decreased from an average of 1.43 to 1.36 s. On termination of microwaves, the temperature decreased to 14.9°C and the ISI increased to an average of 1.56 s. The temperature was then raised with the temperature control unit to 16.1°C. The average ISI decreased to 1.3 s, suggesting that the apparent effect of microwaves on the ISI was a thermal effect. On return to 14.9°C, the average ISI increased to 1.69 s. A 35-second exposure to 476-nm light at 220 minutes stopped the cell's firing for 73 s and, on resumption of spiking, the average ISI had increased to 2.08. The response of the VPN firing frequency to light, then, was the opposite of the response to heat. No change in temperature accompanied the exposure to visible light.

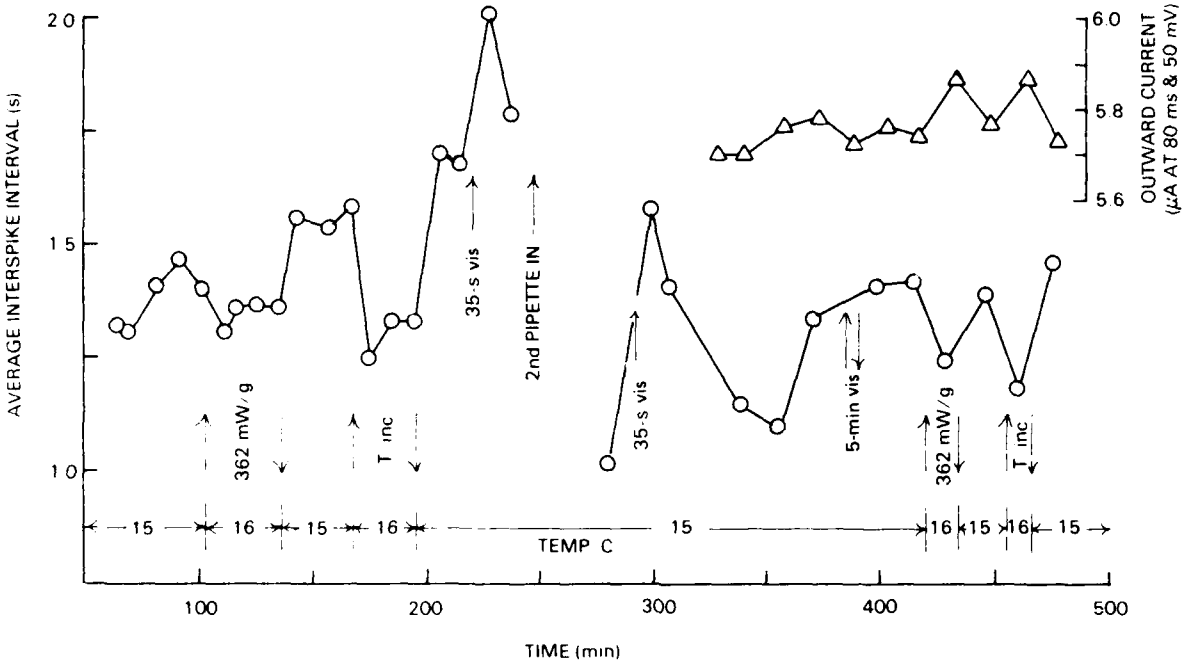

Figure 30. Interspike interval and outward current in VPN, 5-3-84.

The second microelectrode was inserted, and the cell was pulsed and then allowed to recover its beating pattern. Two ISI determinations were made during the recovery period. The cell was spiking faster because of the insertion of the second electrode, and thus the effect of a 35-s exposure to 476-nm light was less than observed previously. Measurements of outward current were begun at 330 minutes. The insert plot in the upper right corner of figure 30 shows the outward current at 80 ms for pulse levels of +50 mV versus elapsed time. Exposure of the cell to 476-nm light, while inhibiting spiking, produced an insignificant change in outward current. On the other hand, microwave exposure with the concommitant increase in temperature, or a temperature change alone, both produced equivalent reversible changes in outward current. Several average ISI determinations were made during the period of outward current measurement and indicate again that microwave exposure accompanied by a temperature increase, or a temperature increase alone, decreased the average ISI in this cell.

Figure 31 illustrates the time course of the ISIs and outward current in another VPN as a function of time and temperature. This cell was not exposed to microwave energy. As the figure shows, increases in temperature induced decreases in average ISI and caused increases in outward current that were reversible on return to the starting temperature of 10.4°C. At the second and third low-temperature interval, the cell was actually silent. Visible light was applied during three of the outward current determinations in this cell, but no discernible change in outward current was observed even though the chart record indicates that an 8 to 10-mV hyperpolarization of the cell occurred during the light exposure.

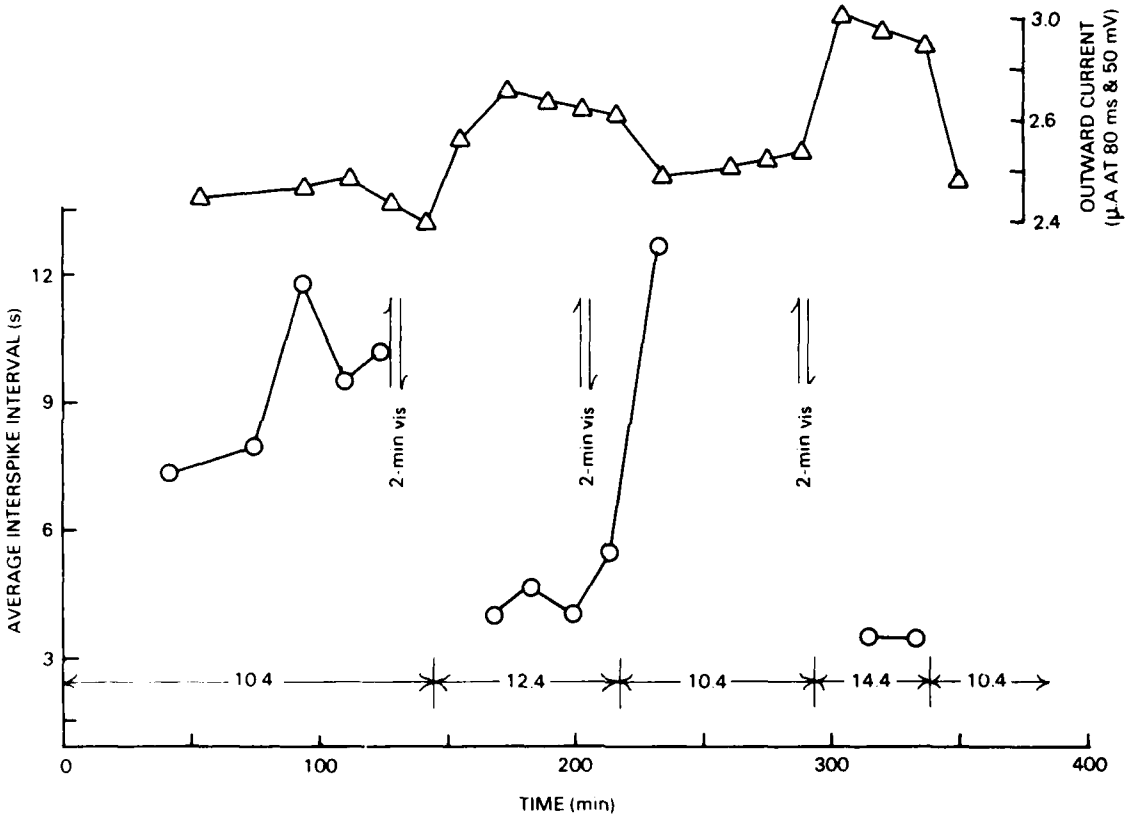

Figure 31. Interspike interval and outward current in VPN, 5-30-84.

These studies with the VPN show that the mechanism of the observed microwave effect on firing frequency was not the same as the mechanism of the light response. The ISI alterations were in opposite directions, and the associated change in late outward current with the microwave exposure did not parallel the lack of change observed with light. In addition, the microwave response

shown in the first cell appears to be primarily a thermal response, since the ISI and outward current changes could be mimicked by increased temperature alone, as demonstrated in both cells.

This finding, however, cannot negate the previously observed (Campbell and Brandt, 1982) microwave-induced ISI responses that were in the same direction as the light response, that of inhibition. And since the dramatic change in ISI induced by light was not accompanied by a change in late outward potassium current, the inhibition induced by microwave energy may likewise not be associated with a change in late outward current. Instead, other membrane currents may be involved.

STATISTICAL ANALYSIS

As indicated above, subjective analysis of late outward current during exposure indicates no apparent effect of microwave energy. To substantiate the hypothesis of no effect, the data were normalized and categorized into time bins in order to sum the data from all cells so that a statistical test could be run. These data consisted of currents measured during the +50-mV pulse and read at 80 ms only. Currents at the +50-mV pulse were considered more informative than currents measured at lower pulse voltages because of the greater accuracy in reading them and their greater sensitivity to changing variables such as temperature and chemicals. The 80-ms read time was chosen since most of the data were measured at 80 ms. The small group of data read at less than 80 ms was not included to ensure similarity in the population of currents studied. Further resrictions on the data used in this analysis were that currents that may have been influenced by another variable other than exposure (such as changing temperature or using Na^+-free seawater) were not included. Therefore, cells subjected to a temperature change or a Na^+-free condition during the 60 minutes preceding exposure, or during exposure, were not included in the analysis. Based on these criteria, data from 14 exposed cells (19 separate exposures) were normalized and classified into time bins. These cells were exposed to between 0.2 and 44 mW/g (1 and 225 mW/cm^2).

Since the protocol called for voltage-clamp series every 15 minutes, time bins were established at 15-minute intervals. The periods preceding exposure were labeled B for 'before.' The periods during exposure were labeled D for 'during,' and the periods after exposure were labeled A for 'after.' The bins were periods centering around 15-minute intervals and were defined as follows:

B0: 0 to 7 minutes preceding exposure
B1: 8 to 22 minutes preceding exposure
B2: 23 to 37 minutes preceding exposure
B3: 38 to 52 minutes preceding exposure
B4: 53 to 67 minutes preceding exposure
B5: 68 to 82 minutes preceding exposure
B6: 83 to 97 minutes preceding exposure

D0: 0 to 7 minutes after initiation of exposure
D1: 8 to 22 minutes after initiation of exposure
D2: 23 to 37 minutes after initiation of exposure

A0: 0 to 7 minutes after cessation of exposure
A1: 8 to 22 mintues after cessation of exposure
A2: 23 to 37 minutes after cessation of exposure
A3: 38 to 52 minutes after cessation of exposure
A4: 53 to 67 minutes after cessation of exposure
A5: 68 to 82 minutes after cessation of exposure
A6: 83 to 97 minutes after cessation of exposure.

The classification of data into bins resulted in each bin of an exposure experiment containing, at the most, one data point.

A further label, Q for 'quick,' was applied when a clamp series occurred within 5 minutes of a previous clamp series. Preliminary analysis of the data indicated that, in most cells, a pronounced drop in late outward currents occurred during clamps following too closely after other clamp series. This may be the result of not allowing enough time either for concentration gradients

to re-establish themselves before clamping again, or for inactivated ion channels to become active again. Since the observed drop in currents may have been the result of insufficient time between clamp series, this type of data was not included in the analysis to determine microwave effects. The Q label had priority over any bin assignment. In other words, data belonging to bin A0 that were labeled Q would not be included in bin A0. During assignment of the data into time bins, all of the D0 data were also Q and all but three of the A0 data were Q. Therefore, none of the data from either of these two time bins was analyzed further.

The magnitudes of late outward currents resulting from +50-mV pulses and read at 80 ms were very different among the different cells studied, ranging from 0.3 to 5.6 μA. Therefore, the data needed to be normalized in order to be combined for statistical analysis. Since the change in currents over time is the relevant datum, the percent change was calculated by using data collected just prior to exposure as a base point. Data in bin B0 were chosen to be the normalizing factor. Data in all other bins of the particular experiment were normalized to B0 by calculating the percent change

$$\frac{(B0) - (X)}{(B0)} \times 100.$$

Analysis then was performed on the percent change in currents over time, and not on the currents themselves.

The results are shown in table 4. As can be seen, there was a trend of decreasing currents after exposure. Microwave energy may have altered the membrane to cause this trend. To further examine this possibility, a similar classification and normalization procedure was performed on control cells - cells not exposed to microwave energy. The criteria for cells to be included in this analysis were the same as those for the exposure group.

Based on these criteria, 20 cells (25 sham exposures) were included in the analysis. Bin classification for the control cells was accomplished by first picking B0 to be about the middle of the experiment such that some data

points could be labeled B, some D, and some A. Once B0 was selected, data assignments into bins were based on time around B0, as specified above. Q labels were also assigned. The results are shown in table 5, where it is seen that the same trend observed in the exposure group is also observed in the control cells. Thus the decreasing outward current following exposure was not the result of microwave energy, but was inherent in the experimental system.

A t-test was performed to examine differences between the exposure and control bins; i.e., the means of exposure D1 was compared to the means of control D1, etc. The results are shown in table 6. No significant ($\alpha = 0.05$) difference was observed.

EFFECT OF TEMPERATURE AND MICROWAVE EXPOSURE

As the experiments progressed and no microwave effects were observed, higher power densities were tried until the microwave exposure caused a change in temperature. Still no effect was observed until the change in temperature exceeded 1.0°C. Because of the cooling system used, this was accomplished only at SARs exceeding 0.35 W/g. The increase in late outward current in these cases was immediate (as was the increase in temperature). The subsequent decrease to pre-exposure levels was within 20 minutes after cessation of exposure (as was the drop in temperature). In each of the three cells exposed to greater than 0.35 W/g, the cell's temperature was also manually altered (during a time of no exposure) and the currents observed. (Data from the VPN studied on 5/3/84 have already been plotted in figure 30 for comparison with the ISI time course but will be re-examined here to emphasize the temperature effect on outward current.)

Table 4. Exposed group percent change from period B0.

Cell	mW/cm^2	B6	B5	B4	B3	B2	B1	B0	D1	D2	A1	A2	A3	A4	A5	A6
307181	100	--	--	10	86	7	3	0	-7	-14	-34	--	--	--	--	--
	100	--	--	--	--	33	11	0	-8	-19	-28	-28	-36	-31	-28	-25
308091	100	0	1	1	2	2	1	0	-2	-3	-3	-5	-6	--	--	--
308151	100	-13	--	-12	-8	--	-5	0	5	20	23	--	--	--	--	--
308241	100	--	31	--	15	2	1	0	5	2	2	0	--	2	2	2
	10	--	--	--	--	--	2	0	-9	--	--	--	3	-6	--	--
308261	100	-12	--	-2	-6	-5	-2	0	-7	-8	-9	-6	-6	--	--	--
	1	--	--	--	-2	-2	-2	0	0	3	0	6	--	--	--	--
	185	--	--	--	--	--	-4	0	-2	-4	-5	-4	--	--	--	--
309071	123	--	0	3	0	0	0	0	0	0	-10	-8	--	--	--	--
309201	212	13	--	7	7	0	0	0	0	0	-4	--	0	-9	-7	--
	222	--	--	--	-2	-2	0	0	0	2	2	--	--	--	--	--
310121	172	--	--	--	--	0	0	0	7	--	7	--	--	--	--	--
310181	178	--	--	--	-2	-2	-1	0	1	1	2	0	2	4	--	--
310201	185	--	--	-4	-2	0	1	0	1	--	4	--	3	4	-18	6
310251	160	--	9	4	1	1	-1	0	1	1	4	7	13	--	13	--
310261	185	--	--	--	--	0	0	0	1	1	0	2	0	1	1	--
402011	143	--	--	--	0	0	0	0	0	0	--	0	0	0	0	0
402071	100	--	--	0	3	1	2	0	-1	1	0	0	1	1	1	--
n		4	4	9	14	16	19	19	19	16	17	12	11	9	8	4
Mean		-3.0	10.3	0.8	6.6	2.4	0.3	0.0	-0.8	-1.1	-2.9	-3.0	-2.4	-3.8	-4.5	-4.3

Table 5. Control group percent change from period B0.

Cell	B6	B5	B4	B3	B2	B1	B0	D1	D2	A1	A2	A3	A4	A5	A6
307261	12	11	9	9	6	-	0	-6	-11	-15	-18	-25	-29	-33	--
	--	--	--	19	10	0	0	--	-14	--	-22	--	-31	--	-34
308011	--	--	--	32	--	13	0	-8	-14	-19	-24	--	--	--	--
	--	--	--	--	--	-41	0	-44	-19	-54	--	--	--	--	--
308221	--	--	--	0	1	0	0	-1	2	--	0	1	--	--	--
	--	--	--	--	--	0	0	0	-1	--	-1	--	--	--	--
308251	--	--	--	--	-1	-1	0	--	6	7	7	7	--	--	--
308311	--	--	--	-8	-2	2	0	--	3	-26	-29	-26	-29	-30	--
309082	--	--	--	--	-20	-6	0	--	-25	-24	--	--	--	--	--
310211	--	--	--	--	--	8	0	17	--	19	--	--	--	--	--
311211	--	--	--	--	5	--	0	--	0	--	-5	--	-5	--	-5
312011	4	--	4	--	0	--	0	--	0	0	--	4	--	4	--
312081	9	--	3	--	0	--	0	--	--	--	0	--	--	0	--
312191	--	--	--	--	18	12	0	0	-3	--	-6	--	0	--	0
401121	--	--	-5	-2	-2	--	0	6	7	--	9	12	--	--	--
401131	--	--	-5	--	--	0	0	--	--	--	3	--	--	--	-3
401161	--	--	--	2	0	--	0	--	-1	0	--	--	--	-12	--
401191	--	--	--	--	-7	-3	0	3	5	6	7	9	--	--	--
401231	--	--	0	--	51	42	0	40	41	--	39	--	39	32	--
401261	--	-4	--	--	--	--	0	2	5	7	--	--	--	--	--
401311	--	--	--	--	-9	-4	0	2	1	--	--	--	--	--	--
403271	--	--	--	0	--	--	0	0	5	2	--	--	--	--	--
404171	--	--	--	--	-3	-2	0	2	5	6	7	--	9	--	--
404231	--	--	--	--	-2	0	0	2	3	5	8	9	14	--	--
405071	--	--	--	--	0	0	0	1	0	0	-1	--	--	--	--
405081	--	4	--	--	--	--	0	2	0	17	--	--	--	--	--
405171	--	--	0	--	--	--	0	6	9	12	--	--	--	--	--
406011	--	--	--	--	-25	--	0	-6	-13	-20	-27	--	--	--	--
n	3	3	7	8	19	17	28	19	25	18	18	8	8	6	4
Mean	8.3	3.7	0.9	6.5	1.1	1.2	0.0	0.9	-0.4	-4.3	-2.9	-1.1	-4.0	-6.5	-10.5

Table 6. Results of t-test comparison of means.

Comparison*	t-statistic
B6 vs CONB6	1.74
B5 vs CONB5	0.78
B4 vs CONB4	0.03
B3 vs CONB3	0.01
B2 vs CONB2	0.34
B1 vs CONB1	0.22
D1 vs COND1	0.48
D2 vs COND2	0.22
A1 vs CONA1	0.26
A2 vs CONA2	0.01
A3 vs CONA3	0.19
A4 vs CONA4	0.02
A5 vs CONA5	0.18
A6 vs CONA6	0.60

*Exposed vs control

Figure 32 shows the time course of the outward current read at 80 ms from the +50-mV pulse for each of the three cells. The percent changes from the immediately preceding point are shown. As can be seen, the change in late outward current during microwave exposure with subsequent change in temperature can be replicated by the changing temperature alone, suggesting that the apparent microwave effect is thermally induced.

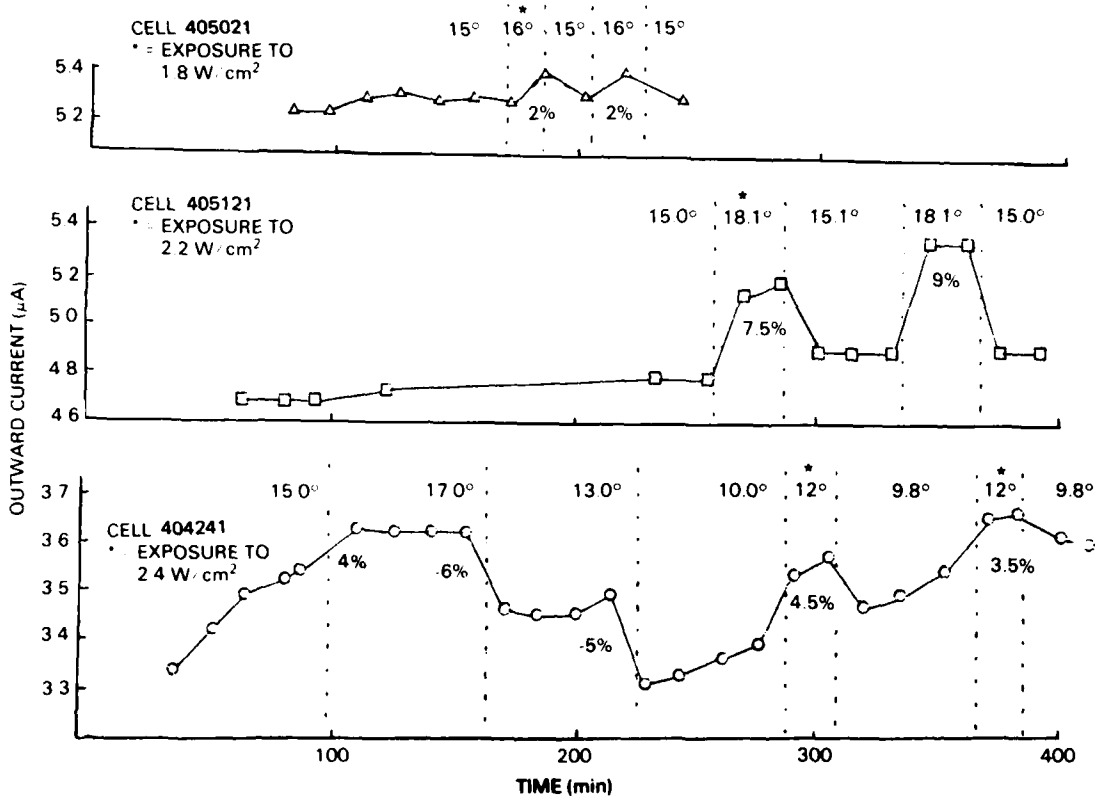

Figure 32. Effect of temperature and microwave exposure on three cells.

A further examination of the effect of temperature on late outward current is shown in table 7, where it is seen that an increase/decrease in temperature caused an increase/decrease in current (except in one cell studied). The amplitude of the percent change of current varied between cells, but was consistent within the same cell. This membrane sensitivity to change in temperature emphasizes the need to maintain temperature control during exposure of microwave energy on neurons.

Table 7. Effect of temperature on late outward current.

Cell	Starting Temperature, °C	Δ Temperature, °C	%ΔI
304281	9.7	+5.6	+90
308151	15.3	-5.3	-27
308241	14.8	-5.1	-65
308301	15.0	-4.8	-7
310261	14.7	-4.7	-17
310311	14.6	-5.0	-2
311091	15.6	-6.0	-23
311211	14.2	-4.1	-15
311233	14.4	-4.6	+3
404171	14.0	-3.8	-6
	10.2	+5.0	+7
404241	15.0	+2.0	+4
	17.0	-4.0	-6
	13.0	-3.0	-5
405021	15.1	+3.0	+9
	18.1	-3.0	-8
405031	14.9	+1.2	+2
	16.1	-1.2	-2
405071	14.9	-4.9	-24
405171	14.9	+2.0	+8

EXPERIMENTS UTILIZING NA^+-FREE ARTIFICIAL SEA WATER (ASW)

Nine cells were subjected to brief (15- to 30-minute) suffusions of Na^+-free ASW, primarily to confirm that inward currents and glitches observed in the current traces of cells were indeed carried by Na^+, and to prepare the system for future work to pinpoint the membrane channel(s) responsible for any microwave-induced current alteration. In one case during a more prolonged suffusion with Na^+-free ASW, the cell was exposed to 2.45-GHz energy. The exposure resulted in a previously unobserved outward current peaking at about 6 ms. Figure 33a illustrates the current traces in Na^+-free ASW and figure 33b the appearance of the unusual outward current during microwave exposure. Figure 33c shows the current following exposure and 20 minutes after return to sea water. While the unusual outward current is still detectable, its magnitude has diminished. Two other attempts to elicit this current in Na^+-free ASW-suffused cells were unsuccessful.

DISCUSSION

The goals of this study were to observe changes in membrane ionic currents during microwave exposure. It was expected at first that several currents could be examined, most specifically voltage-dependent early-inward Na^+ current, voltage-dependent late-outward K^+ current, and voltage-dependent inward Ca^{++} current. However, the Na^+ current was not analyzed because of its quick onset and thereby its overlapping with capacitive currents. The inhibition of the opening of these channels would cause a decrease in firing frequency, as has been observed during microwave exposure. The Na^+ channels then may still be the site of microwave interaction, and should be further studied on systems designed for strict minimization of capacitive current.

The late-outward K^+ current was quantified and analyzed as discussed in Results, above. No effect of microwave exposure was observed.

The waveshape of the membrane current response to a clamp pulse was examined for alterations during exposure. Often, a noticeable segment of this waveshape represented inward Ca^{++} current. It was expected that any observed change in the membrane current waveshape would be analyzed as to the

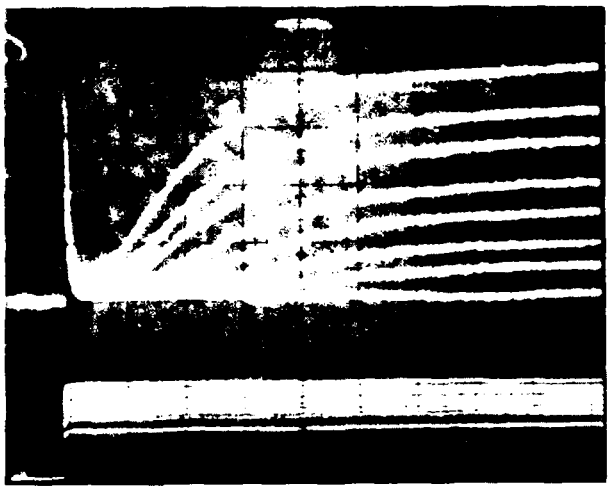

a. Na^+-free artificial sea water.

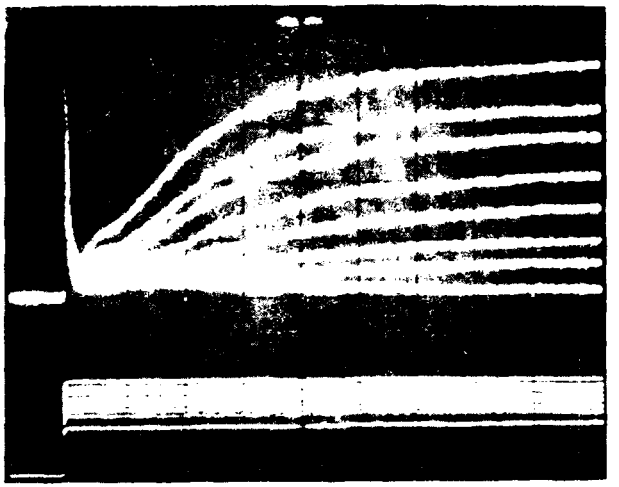

b. In Na^+-free artificial sea water, with exposure.

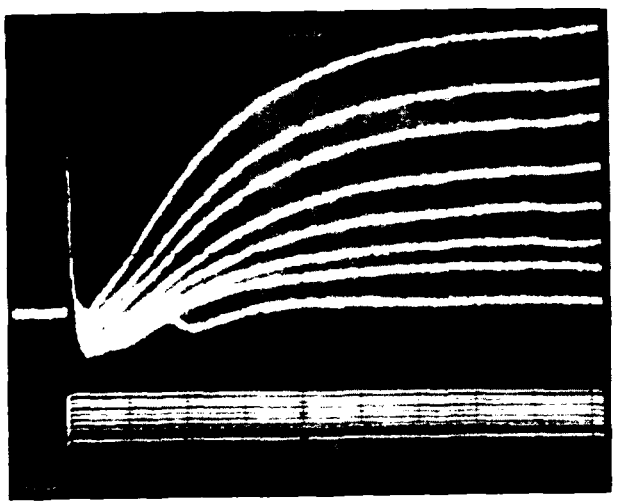

c. In sea water 20 minutes after exposure.

Figure 33. Appearance of an outward current at 6 ms in Na^+-free artificial sea water during exposure (19.6 mW/g).

particular ionic channel involved. Pharmaceuticals would then be added to the sea water to block the suspected channel(s), resulting in an additive or subtractive influence on the microwave effect. The site(s) of the microwave interaction would then be known. However, in this study no alteration of the waveshape was observed, so no follow-up pharmaceutical studies were begun.

Nevertheless, it is believed that pharmaceuticals, by blocking channels that may mask alterations of other currents, can also make the voltage clamp system more sensitive to the study of microwave effects. This increased sensitization may have been occurring when a new outward current peak was observed during microwave exposure in the presence of Na^+-free ASW [see Experiments Utilizing Na^+-free Artificial Sea Water (ASW), above]. Combining the effect of an altered ion environment with microwave exposure, and using voltage clamping to detect interactions, may yield the membrane mechanism of the microwave effect that was not observable in this study. Future studies should consider this approach.

CONCLUSIONS

1. Firing patterns can correspond to membrane current patterns.

2. Changes in firing patterns do not have to be associated with a change in late outward K^+ current.

3. Microwave energy does not affect late outward K+ current (unless accompanied by a temperature change).

4. Alteration of the cell's ionic environment with ASW or channel inhibitors may sensitize the voltage-clamp system to microwave effects.

REFERENCES

Adams, D.J., S.J. Smith, and S.H. Thompson, Ionic Currents in Molluscan Soma, Ann Rev Neurosci 3:141-167, 1980.

Allis, J.W., C.F. Blackman, M.L. Fromme, and S.G. Benane, Measurement of Microwave Radiation Absorbed by Biological Systems, 1, Analysis of heating and cooling data, Radio Sci 12(65):1-8, 1977.

Andresen, M.C., and A.M. Brown, Photoresponses of a Sensitive Extraretinal Photoreceptor in Aplysia, J Physiol (London) 287:267-282, 1979.

Arber, S., The Effect of Microwave Radiation on Passive Membrane Properties of Snail Neurons, J of Microwave Power 16(1): 15-20, Mar 1981.

Arber, S.L., and J.C. Lin, Microwave Effects on Helix Aspersa Neurons, Abstract, 4th Annual Scientific Session of Bioelectromagnetics Society, held in Los Angeles, CA, 28 Jun-2 Jul 1982.

Arber, S.L., and J.C. Lin, Role of External Calcium in Microwave-Induced Snail Neuron Response, Abstract, 5th Annual Scientific Session Bioelectromagnetics Society, held at the University of Colorado, Boulder, 12-17 Jun 1983.

Arvanitaki, A., and N. Chalazonitis, Patterned Activities from Identifiable "Cold" and "Warm" Giant Neurons (Aplysia), Proc of the First Int'l Symp on Olfaction and Taste, Pergamon Press, NY, p 377-380, 1963.

Campbell, N.L., and C.L. Brandt, Mechanism of Electromagnetic Energy Effects on the Nervous System; Experimental System and Preliminary Results, Technical Report 698, Naval Ocean Systems Center, San Diego, CA, 1 Jul 1982.

REFERENCES (Continued)

Connor, J.A., and C.F. Stevens, Prediction of Repetitive Firing Behavior from Voltage Clamp Data on an Isolated Neurone Soma, J Physiol (London) 213:31-53, 1971.

Frazier, W.T., E.R. Kandel, I. Kupfermann, R. Waziri, and R.E. Coggeshall, Morphological and Functional Properties of Identified Neurons in the Abdominal Ganglion of Aplysia californica, J Neurophysiol 30:1288-1351, 1967.

Kandel, E.R., Cellular Basis of Behavior, W.H. Freeman, San Francisco, CA, 1976.

Lin, J.C., and S.L. Arber, Response of Snail Nerve Cells to Noise Modulated Microwave Field, Abstract, 4th Annual Scientific Session of Bioelectromagnetics Society, held in Los Angeles, CA, 28 Jun-2 Jul 1982.

Ogden, T.E., M.C. Citron, and R. Pierantoni, The Jet Stream Microbeveler: An Inexpensive Way to Bevel Ultrafine Glass Micropipettes, Science 201:469-470, 1978.

Seaman, R.L., and H. Wachtel, Slow and Rapid Responses to CW and Pulsed Microwave Radiation by Individual Aplysia Pacemakers, J of Microwave Power 13(1):77, 1978.

Sheppard, A.R., and W.R. Adey, Use of Time Series Analysis for the Detection of ELF Electric Field Effects on Neuronal Firing Rates, Abstract, 4th Annual Scientific Session of Bioelectromagnetics Society, held in Los Angeles, CA, 28 Jun-2 Jul 1982.

Thompson, S.H., Three Pharmacologically Distinct Potassium Channels in Molluscan Neurons, J Physiol (London) 265:465-488, 1977.

Wachtel, H., R. Seaman, and W. Joines, Effects of Low-Intensity Microwaves on Isolated Neurons, New York Acad of Sciences 247:46, 1975.

END

FILMED

3-86

DTIC